` ***Title page***

Long-term excess nitrogen fertilizer increases sensitivity of soil microbial community to seasonal change revealed by ecological network and metagenome analyses

Bing-Bing Li[a, b, c, d], Sarah S. Roley[e, g], David S. Duncan[f], Jiarong Guo[c, d], John F. Quensen[c, d], Han-Qing Yu[b, *] and James M. Tiedje[c, d, *]

[a] School of Life Sciences, University of Science & Technology of China, Hefei 230026, China

[b] CAS Key Laboratory of Urban Pollutant Conversion, Department of Environmental Science and Engineering, University of Science & Technology of China, Hefei 230026, China

[c] Department of Plant, Soil and Microbial Sciences, Michigan State University, East Lansing, Michigan 48824, USA

[d] Center for Microbial Ecology, Michigan State University, East Lansing, Michigan 48824, USA

[e] Great Lakes Bioenergy Research Center and W.K. Kellogg Biological Station, Michigan State University, Hickory Corners, Michigan 49060, USA

[f] Department of Agronomy, University of Wisconsin, Madison, Wisconsin 53706, USA

[g] Current address: School of the Environment, Washington State University, Richland WA 99354

*Address correspondence to James M. Tiedje and Han-Qing Yu:

Department of Plant, Soil and Microbial Sciences, Michigan State University, East Lansing, Michigan 48824, USA. E-mail: tiedjej@msu.edu

CAS Key Laboratory of Urban Pollutant Conversion, Department of Environmental Science and Engineering, University of Science & Technology of China, Hefei 230026, China. E-mail: hqyu@ustc.edu.cn

ABSTRACT

Nitrogen (N) fertilizer has often been generously applied to increase crop biomass yield. Although the influences of inorganic N fertilizer on soil microbial communities have been widely studied, the effect of N fertilizer on microbial co-occurrence networks and its metagenome is largely unknown. Further, seasonal changes in microbial community responses to N addition have rarely been reported. In this study, three N fertilizer rates (0, 56, 196 kg N/ha) were applied annually in switchgrass (*Panicum virgatum* L.) grown for bioenergy production in the upper Midwest, USA. The soil microbiome was affected by both fertilizer and low pH in the 7^{th} year of fertilization treatments. The microbial community structures were relatively stable during the growing season for each N fertilizer rate. However, the excess N fertilizer (196N) increased the seasonal variation of bacterial and fungal communities. Network analysis showed that the microbial interactions at the 196N treatment were more intense, with decreased bacteria-fungal interactions compared to 56N and 0N. This suggests that the microbial community became more sensitive to environmental change under the influence of long-term excess N fertilizer. Metagenomic analysis showed that the long-term excess N fertilizer promoted many metabolic processes, especially carbohydrate and amino acid related metabolism and Archaea mediated ammonia oxidation. However, N fertilizer also reduced many other traits, especially N_2 fixation and signal transduction, the latter of which may contribute to the decreased interactions between bacteria and fungi.

Keywords: Soil microbiome; Nitrogen fertilizer; Growth stage; Ecological network; Soil metagenome

1. Introduction

Numerous studies have demonstrated that long-term application of inorganic nitrogen (N) fertilizer can reduce species in the aboveground plant community, acidify the soil, increase nitrous oxide emissions, decrease N_2 fixation potential, and undermine ecological sustainability (c.f., Geisseler and Scow, 2014; Roley et al., 2018; Ruan et al., 2016). Microorganisms mediate biogeochemical cycles of C, N, and other elements, and as a result, the microbial community can be impacted by N fertilizer in several ways. For example, N fertilizer can indirectly influence the microbial community through altering the plant community and acidifying soil (Hu et al., 2017; Meier and Bowman, 2008; Zeng et al., 2016). The microbial community is also impacted directly by increased soil N availability through inhibiting enzyme activities and shifting community composition (Fierer et al., 2012a; Gallo et al., 2004; Paungfoo-Lonhienne et al., 2015; Yan et al., 2017). Grass roots, important in this study, are widely and deeply distributed in soil, changing the microbial environment by providing carbon and also affecting oxygen, nutrients, moisture, and pH. Further, the organic compounds secreted by roots influence the microbial community and those compounds vary seasonally with root age (Aulakh et al., 2001; Badri and Vivanco, 2009; Lucas García et al., 2001). As a result, we postulate that microbial communities will be influenced by interactions between N fertilizer and season.

In addition to the physicochemical environment, microorganisms are influenced by community interactions, including those between bacteria and fungi. Bacteria and fungi almost always cohabit the same environment, and various substances and energy exchanges inevitably occur between them (Benoit et al., 2015; De Boer et al., 2005; Warmink et al., 2009). For example, *Bacillus subtilis* adheres to the mycelium of fungi in the presence of the fungus

Aspergillus niger (Benoit et al., 2015). Most of the current research about the interaction between bacteria and fungi was carried out in the laboratory and focused on the interaction between a few microorganisms. In the natural environment, the types and quantities of microorganisms are abundant, and the external factors are complicated, making the laboratory results difficult to apply. In recent years, more studies have been conducted in natural samples describing the coexistence between bacterial and fungal communities. Network-related analysis of the terminal-restricted length polymorphism data showed that bacterial and fungal communities and soil properties were related to each other as seen in a typical correlation module (De Menezes et al., 2015). Community networks and interactions also vary with environmental conditions. Ma et al. (2016) described geographic distribution characteristics of a soil microbial coexistence network topography in eastern China and found that community network characteristics changed in different climate zones. The addition of straw reduced the negative correlation between bacteria and fungi in the soil, suggesting that competition between microbes dominated in nutrient scarce environments (Banerjee et al., 2016). In short, coexistence characteristics within microbial communities exist in an array of environments and are affected by a variety of environmental factors, but the effect of N fertilizer has not been sufficiently explored relative to its extent of use. Based on the previous results, we hypothesize that N fertilizer will affect community network characteristics and decrease negative interactions between microbes because N addition may alleviate competition.

Soil metagenomic analyses now provides the opportunity to go beyond community structure descriptions to study functional attributes, like N processes, as well as to assemble genomes (Fierer et al., 2012b; Nelson et al., 2016; Orellana et al., 2017). N fertilizer addition can increase DNA/RNA replication, electron transport, and protein metabolism-related genes (Fierer

et al., 2012a) and increase the relative abundances of genes associated with carbohydrate metabolism (Leff et al., 2015). Fertilizer responses may vary by taxon; genomes assembled from metagenomes indicated that archaeal ammonia oxidizers may respond faster than other recovered population genomes to N fertilization (Orellana et al., 2017). Microbial community composition, community interactions, and function are thus likely to shift in response to N fertilizer addition. Deeper metagenomic sequencing will reveal shifts in N cycle genetic capacities due to N fertilization and test those relationships with their functions.

We sought to examine the long-term effect of N fertilizer addition on bacterial and fungal community interactions and function across seasons. Our objectives were to 1) determine the extent of the bacterial and fungal community shifts with N fertilizer addition; 2) assess the seasonal responses of bacterial and fungal communities to switchgrass growth stage in conjunction with N fertilizer addition; 3) elucidate the effect of N fertilizer on microbial co-occurrence networks; and 4) compare the metabolic potential of microbial communities between unfertilized and fertilized soil samples by metagenomic analyses.

2. Materials and Methods

2.1. Sampling site description

Switchgrass (*Panicum virgatum* L.), is a perennial grass, native to North America prairies and steppes. In 1991, U.S. Department of Energy selected it as a model biomass crop for liquid biofuels (Monti, 2012; Parrish and Fike, 2005). A manipulative experiment was established in the upper Midwest, USA to test the response of switchgrass yields to N fertilizer addition and

94 establish optimal fertilizer levels (Ruan et al., 2016). The switchgrass N rate experiment is part
95 of the Great Lakes Bioenergy Research Center (GLBRC) and located at the Kellogg Biological
96 Station (KBS) in Michigan (42°23′ N, 85°22′ W). Plots were established in 2008, with the
97 fertilization experiment established in 2009. Eight N fertilizer rates (0, 28, 56, 84, 112, 140, 168,
98 196 kg N ha^{-1} $year^{-1}$) were applied once per year as urea-ammonium-nitrate (28% N solution).
99 The original goal of the switchgrass N rate experiment was to determine optimal fertilizer levels
100 for annually-harvested switchgrass; the wide range (unfertilized to rates used on row crops)
101 ensured the optimal rate would be captured.
102 At KBS, the predominant soil series is Kalamazoo loam (Fine-Loamy, Mixed,
103 Semiactive, Mesic Typic Hapludalfs). Detailed information about the experimental design, and
104 rates of N_2 fixation, net nitrification, net ammonification, field denitrification, and N_2O
105 production were reported for the same samples used in this study (Roley et al., 2018). The mean
106 annual temperature (MAT) and mean annual precipitation (MAP) between 1981 and 2010 were
107 9.9 °C and 1,027 mm, respectively (Sanford et al., 2016). Climate information for the year of the
108 experiment, 2015, is in Table S1. Aboveground biomass was harvested annually after
109 senescence, removing over 90% of the above ground biomass so that aboveground plant nitrogen
110 and carbon were not returned to the soil. The switchgrass showed little to no yield response to N
111 fertilizer over the 2013 to 2016 seasons, a pattern observed in other switchgrass plots, as well
112 (Fike et al. 2017, Wang et al. 2019) potentially because of recently-fixed N (Roley et al., 2018).
113
114 *2.2. Soil sampling and DNA extraction*
115

Soil samples were collected from each of four replicates of three N fertilizer treatments: 0, 56 and 196 kg N ha^{-1} $year^{-1}$, designated as 0N, 56N, and 196N, respectively. The 0N and 196N treatments represent lowest and highest N rates in the switchgrass N rate experiment, while the 56N treatment is the recommended agronomic rate that corresponds to the amount of N expected to be removed during harvest (the replacement value). Sampling occurred four times in 2015 during key timepoints, yielding 48 samples. Key timepoints included prior to fertilization (emergence of switchgrass, May 11), two or three weeks since fertilizer addition (early growth of switchgrass, June 1), at plants' peak productivity stage (July 20), and after senescence (October 13).

Soils were collected with a hammer core (dimensions: 15 cm × 5 cm). Each core was between 3 and 5 cm from a switchgrass crown, and thus included a mixture of bulk and rhizosphere soil. Soil from the cores was placed in plastic bags and kept on ice after collection and during transportation. Soils were sieved through a 4-mm sieve, with roots removed and then stored at –20 °C in the laboratory until further processing.

DNA was extracted from 0.5 g of the mixed soil sample using the Powersoil DNA Extraction kit (MOBIO Laboratories, Carlsbad, CA, USA) following the manufacturer's instructions. DNA quality and concentration were measured by Nanodrop (Thermal) and Qubit kit (Life Technologies), respectively. Polymerase chain reactions (PCR) were also performed to check if the DNA could be amplified by universal primer pairs of 515f-806r for bacteria and fITS9-ITS4 for fungi (Apprill et al., 2015; Ihrmark et al., 2012).

2.3. Measurement of soil characteristics

Ammonium and nitrate were measured on soil from the same core as the DNA extractions, and pH was determined on an adjacent 15-cm core, collected at the same time. Total carbon and total nitrogen were determined after senescence. Inorganic soil nitrate and ammonium concentrations were determined after extracting a 10-g subsample with 100 mL of 1 M potassium chloride, shaking for 1 min, resting for 24 h, and then shaking again for 1 min. Nitrate and ammonium concentrations were measured on the filtered supernatant using a Lachat QuikChem 8500 flow injection analyzer (Hach, Loveland, CO) (Robertson et al., 1999). Total carbon and total nitrogen were determined on oven-dried soil via dry combustion on an elemental analyzer (Costech ECS 4010, Valencia, CA, USA). Soil pH was determined with a glass electrode in a 1: 2 slurry of air-dried soil in 0.01 M $CaCl_2$.

2.4. Quantification of bacterial and fungal abundances

Bacterial and fungal abundances were quantified by quantitative polymerase chain reaction (Q-PCR). Primer sets of 515f-806rB and FR1-FF390 were used to assess the abundances of bacteria and fungi, respectively (Apprill et al., 2015; Chemidlin Prevost-Boure et al., 2011). Q-PCR was conducted using Power SYBR Green PCR Master Mix (Applied Biosystems, Warrington, UK) in Applied Biosystems (ABI) 7900HT sequence detection system. A total of 10 μL PCR reaction volume per well contained 5 μL SYBR Green mastermix, 0.4 μL forward and reverse primers (10 μM), 3.7 μL PCR H_2O and 0.5 μL soil DNA with concentration of less than 10 ng/μL. Standard curves were obtained with the serial dilutions of plasmid DNA containing the target genes, which were amplified from soil DNA by 515f-806rB and FR1-FF390, respectively. Then, the PCR amplified fragments were cloned using the pGEM-T vector

(Promega Corp. Madison, WI USA) according to the manufacturer's instruction. Several positive clones were sequenced to make sure that correct fragments were amplified by these two primer sets. Standard PCR condition was applied for 16S rRNA gene: 2 min of denaturation at 50 °C, 10 min of polymerase activation at 95 °C, followed by 40 cycles of 15 s at 95 °C, 1 min at 60 °C. The PCR condition for ITS2 gene was 2 min of denaturation at 50 °C, 10 min of polymerase activation at 95 °C, followed by 40 cycles of 15 s at 95 °C, 30 s at 50 °C and 1 min at 72 °C.

2.5. Amplification and Illumina Miseq sequencing

Primer set 515f-806rB was used to amplify bacterial and archaeal V4 regions of 16S rRNA genes, and primers fITS9 and ITS4 were used to amplify the fungal internal transcribed spacer (ITS2) according to previously published protocols (Apprill et al., 2015; Ihrmark et al., 2012). All primer sets contained Illumina linkers, a 12bp barcode index, a pad region, a 0,1,2 or 3 base pair long spacer and the sequence-specific primer. All the amplicons were pooled together, cleaned and bi-directionally sequenced on the Illumina Miseq platform. Sequencing was performed at DOE Joint Genome Institute, Walnut Creek, California, USA. Bacterial and fungal raw reads were deposited in the NCBI Sequence Read Archive (SRA) database under accession numbers PRJNA628034 and PRJNA628127, respectively.

2.6. iTag sequence processing

Raw sequences were sorted according to barcode and assembled through the RDP modified pandaseq with low quality (Q score <25) and short reads (length <200) removed.

Primers were removed through RDP SeqFilters tool (Cole et al., 2014). All the 16S rRNA gene reads were classified using RDP naive Bayesian classifier (Wang et al., 2007) after chimeras were filtered using UChime (Edgar et al., 2011). For ITS reads, the ITS2 regions were extracted by ITSx software (Bengtsson-Palme et al., 2013) followed by RDP naive Bayesian classifier against the Warcup reference database available through RDP. All samples of 16S rRNA gene reads and extracted ITS2 regions were subsampled to the same sequence depth before classification, with 77,858 sequences and 105,266 sequences, respectively. Both the clean 16S rRNA gene reads and extracted ITS2 regions were clustered by using the UPARSE pipeline (Edgar, 2013) of the USEARCH V8 (Edgar, 2010) at 97% nucleotide identity for both genes.

2.7. Co-occurrence network construction

An integrated OTU table of both bacterial and fungal OTUs was used to construct networks for each of the three N fertilizer rates, producing three networks. Each network was constructed by calculating the co-occurrence among 16 replicates except for one network with 15 replicates. Both bacterial and fungal OTUs with average relative abundances less than 0.01% were removed from each integrated OTU table. OTUs with a relative abundance of zero in more than eight replicates were also removed. The computation of pairwise similarity matrix was based on Spearman correlation with *P*-value adjusted using FDR method. The same similarity threshold (St) (0.880) was set for networks construction to make sure the three networks were comparable. The St of 0.880 was stricter than adjusted *P*-value less than 0.05. The nodes and links could be drawn in the undirected network, as long as the adjacent matrix was determined. All analyses were finished on the molecular ecological network analysis pipeline platform

(MENA, http://ieg2.ou.edu/MENA/) (Deng et al., 2012). Gephi 0.9.2 software was used to draw networks (Bastian et al., 2009).

We describe the characters of modules in each network. One module represents a group of nodes, which are highly interconnected and interacted less with other nodes. Modules in the networks were searched by a greedy modularity optimization method. Modularity (M) describes the degree to which a network is divided into modules. Modular structure was defined by using $M > 0.4$ as threshold. Connectivity of each node was determined by connectivity within module (Zi) and connectivity among module (Pi). Nodes can be classified based on Zi and Pi values according to the topology roles they played in the network. There are four types of topology for nodes, which are module hubs ($Zi > 2.5$), network hubs ($Zi > 2.5$ and $Pi > 0.62$), connectors ($Pi > 0.62$) and peripherals ($Zi < 2.5$ and $Pi < 0.62$). N fertilizer sensitive OTUs, whose abundances were significantly varied between different N fertilizer rates, were further identified as indicator species by both R package *indicspecies* (De Cáceres et al., 2010) ($P < 0.05$) and package *edgeR* (Robinson et al., 2010) ($P < 0.05$), and were displayed in meta co-occurrence network of all N fertilizer rates. Meta network was constructed based on strong Spearman correlations ($\rho > 0.5$ and $P < 0.001$, adjusted p-value using FDR method) between bacterial and fungal OTUs (average relative abundance > 0.01%) in all samples by R package *igraph* (Csardi and Nepusz, 2006) with the Fruchterman-Reingold layout (10^4 permutations).

2.8. Shotgun Hiseq sequencing

The unfertilized sample (0N) and excess fertilized sample (196N), each with four replicates, at plant peak productivity stage were subject to shotgun (metagenomics) sequencing.

The sequencing was conducted on the Illumina Hiseq 2500 platform at DOE Joint Genome Institute. Each sequencing library was prepared by Illumina's Truseq library kit following the standard procedure of the manufacturer. Briefly, genomic DNA was randomly sheared by sonication into fragments of 100-300 bp by sonication with those of about 200 bp selected by SPRI (Solid Phase Reversible Immobilization) technology (DeAngelis et al., 1995). The termini of selected fragments were repaired, poly(A) tails were added and adaptors of paired-end sequencing were linked. The prepared libraries were then sequenced, one lane per sample to obtain greater sequencing depth. The raw sequencing data of 0N and 196N samples can be accessed under consecutive numbers from PRJNA406038 to PRJNA406045 in the SRA of NCBI.

2.9. Metagenomic data processing and annotation

The adaptors in raw reads were removed through BBDuk adapter trimming software (https://sourceforge.net/projects/bbmap/) (Bushnell, 2015). The reads were then filtered and trimmed by BBDuk program. Reads with quality scores lower than 12, containing more than three "N", or with average quality score lower than 3, with length shorter than 51 bp and those reads matching the Illumina background sequences (artifact, spike-ins or phiX) were all removed. The remaining reads were later mapped against human reference genome HG19 by BBMap and the reads with > 93% similarity to human HG19 genome were trimmed. MEGAHIT assembly tool was adopted to assemble high quality reads (Li et al., 2015). The default sizes of Kmer were used, i.e., 23, 43, 63, 83, 103 and 123. The coverages of assembled contigs were obtained by mapping the assembled contigs against raw reads with high quality. COG, Pfam and

KEGG databases were used for functional gene annotation with HMMER 3.1b2 (Eddy, 2011; Finn et al., 2016; Kanehisa et al., 2016; Tatusov et al., 2003). A parallel annotation was performed on MG-RAST platform (Lees et al., 2014). The assembled contigs were directly uploaded to MG-RAST platform. The contigs with length > 500 kb were removed and the abundance information of each contig was appended to the end of the sequence name before uploading. Information about functional genes and microbial community composition were obtained from MG-RAST SEED subsystems database.

The assembly and annotation of N cycle genes was conducted by Xander software (Wang et al., 2015). The forward reads and reverse reads produced from pairwise end sequencing were split. Secondly, two sets of reads were quality controlled and adaptors were trimmed by Trimmomatic software (Bolger et al., 2014). The reference file of each N cycle gene was built by well-known gene sequences, protein sequences, and HMMER 3.0 program following the software instructions. The N cycle genes were then assembled and annotated based on reference files and trimmed raw reads. RDP has the reference databases for archaeal (AOA) and bacterial (AOB) ammonia monooxygenase subunit A genes (*amoA*), nitrogenase gene (*nifH*), nitrite reductase genes (*nirK* and *nirS*), nitric oxide reductase genes (*norB_cNor* (a cytochrome bc-type complex) and *norB_qNor* (encodes the quinol-oxidizing single-subunit class)), nitrous oxide reductase gene (*nosZ*), and 50S ribosomal subunit protein L2 gene (*rplB*). The *rplB* gene is a single copy housekeeping gene, which is used to standardize the relative abundance of N cycle genes (Wang et al., 2015).

2.10. Statistical analysis

Downstream statistical analyses were mainly performed in R (version 3.2.2; https://www.r-project.org). Alpha-diversity (Shannon diversity, species richness and Pielou's evenness) was calculated according to the OTU table with VEGAN package (version 2.4-2; https://github.com/vegandevs/vegan) (Dixon, 2009). Weighted UniFrac distance based principal coordinate analysis (PCoA) was performed using GUniFrac, ade4 and VEGAN packages to illustrate the beta-diversity between treatments. The "envfit" function in VEGAN was applied to fit environmental factors onto PCoA ordination. Fold change between two groups at the genus level was calculated using DESeq package. The significantly changed genera ($|\log_2 \text{fold change}| > 1$, P value < 0.05, mean relative abundance > 0.1%) were selected and displayed on heatmaps. Heatmap plots were drawn by "pheatmap" package with relative abundance of genus scaled. The box plots, dot plots, and bar plots were generated using "ggplot2" package (version 2.2.1) (Wickham, 2009). Spearman correlation between alpha diversity indexes and environmental factors and significance test were performed with "Hmisc" package. To determine the significance of differences, one-way analysis of variance (ANOVA) followed by the Tukey's HSD test was performed with AGRICOLAE package (version 1.2-1; https://cran.r-project.org/web/packages/agricolae). Permutational multivariate analysis of variance (PPERMANOVA) analysis was conducted to test the effects of site, fertilization, growth stage, and their interaction on microbial community structure using "adonis" function in VEGAN package.

3. Results

3.1. Physicochemical properties of soil samples

As indicated in Table S1, after replacement rate of fertilizer (56N) was applied at the site, the ammonium and nitrate were rapidly assimilated decreasing the values to the deficiency fertilizer rate (0N) in about 2 weeks. The ammonium and nitrate concentrations remained at the same level as 0N sample for the remainder of the growing season, except for the excess (196N), where both ammonium and nitrate concentrations increased after fertilization. The soil pH with the 196N fertilizer treatment was significantly lower, with a pH of 4.93 compared to a pH of 6.35 in the 0N plot, and the reduced soil pH remained stable during the growing season. The addition of 56N and 196N fertilizers did not show a lasting effect on the soil ammonium and nitrate concentrations.

3.2. Bacterial and fungal abundance

The bacterial abundance decreased significantly after the 196N fertilizer application, with a big difference in bacterial abundance noted between the 0N and 196N samples at peak productivity stage [$(8.25\pm5.48)\times10^7$ vs $(3.01\pm1.68)\times10^6$ copies/g soil, respectively] (Fig. S1). The fungal abundances were relatively similar among the three N application rates, and it was extremely stable throughout the growing season.

3.3. Seasonal variations of bacterial community diversity and composition across N gradient

Notably, the three alpha diversity indexes (Pielou's evenness, Shannon diversity, Species richness) of bacterial communities were strongly decreased by 196N fertilizer (Fig. S2A, dark red bar). The three diversity indexes were strongly and positively correlated with each other and

323 pH was significantly associated with all diversity indexes (Table S2). The three diversity
324 indexes, however, were generally stable across the growing season for each fertilizer rate,
325 although with minor significant fluctuations, especially the 196N treatment which showed
326 increased variation at senescence (Fig. S2A, dark red bar).
327 Similar impacts of N fertilizer on bacterial beta diversity, as seen for alpha diversity,
328 were observed (Fig. 1A, S3A, S4A), where the bacterial community structure was significantly
329 affected by 196N fertilizer at each growth stage ($P = 0.003$, $P < 0.001$, $P = 0.01$ and $P = 0.007$
330 for pre-fertilization, post-fertilization, peak productivity, and senescence, respectively) (Fig.
331 S3A, pink indicator, Table S3). The bacterial community structure of each fertilizer treatment
332 was stable across the growing season (Fig. 1A, S3C, Table S3). We also found that the Unifrac
333 distance between growth stages for bacterial communities of the 196N treatment was
334 significantly larger than those of 0N and 56N (Fig. 2B, ***$P < 0.001$). At the phylum level,
335 *Proteobacteria* and *Acidobacteria*, the two dominant phyla, were not impacted by fertilizer (Fig.
336 S4A). The absence of change at the higher taxonomic level can mask changes at a lower level,
337 e.g. some subgroups of *Acidobacteria* phylum (Gp1, 3, 4, 6, 16) and subgroups of
338 *Proteobacteria* were significantly affected by excess N fertilizer (Fig. S4B, Fig. S5A). However,
339 the genera which were significantly affected by growth stage were rarely detected.
340
341 *3.4. Seasonal variations of fungal community diversity and composition across N gradients*
342
343 Fungal community alpha and beta diversities varied greatly across the N fertilizer
344 gradient and switchgrass growth stage (Fig. S2B, 1B, S3(B, D)). The dissimilarity Unifrac
345 distance between fungal communities was about twice that of bacteria for the same samples (Fig.

346 2). The variation between replicates of fungal communities was also larger than that of bacteria
347 (Fig. 2, S5B). N fertilizers significantly affected the fungal community at post-fertilization, but
348 this significant effect was attenuated during the season (Fig. S3B, Table S4). In addition, we
349 didn't find an obvious effect of growth stage on fungal community structure for each fertilizer
350 rate (Fig. 1B, S3D), and growth stage explained a very small variation of microbial communities
351 (Fig. S6). The Unifrac distance between growth stages for fungal communities of 196N samples
352 was also found to be significantly larger than those of 0N and 56N samples (Fig. 2D, $*P < 0.05$).
353 For fungal community composition, there were obvious differences between unfertilized samples
354 and fertilized samples at phylum and class levels (Fig. S4C and D). Highly affected fungal
355 genera varied greatly across N fertilizer gradient and switchgrass growth stage. The arbuscular
356 mycorrhizal fungi (AMF) community was severely inhibited by N fertilizer (Fig. S5).
357
358 *3.5. Co-occurrence of bacteria and fungi by network analysis*
359
360 We integrated samples from different growth stages from each N fertilizer rate to
361 construct three networks. As shown in Table 1, high value of R^2 of power-law ($R^2 > 0.838$) in
362 this study indicated the scale-free property of the three networks. The values of avgCC, HD and
363 modularity ($M > 0.4$) in empirical networks were higher than those in random networks,
364 indicating small-world and modularity properties. Therefore, the networks constructed in this
365 study can be used to reveal the response of microbial co-occurrence to N fertilizer, similar to
366 previous literature (Deng et al., 2016; Shi et al., 2016; Zhou et al., 2011).
367 The 196N network had highest avgK, avgCC, and density, and lowest HD values (Fig.
368 3A, Table 1). The 56N network had lower avgK and avgCC, and highest HD values (Table 1).

The 196N fertilizer rate reduced the interaction between bacteria and fungi, but significantly increased the percentage of positive links between microorganisms to 87.9% under the influence of long-term fertilization (Fig. 3A, Table 1). Moreover, the relative numbers of fungal nodes were also reduced in 196N samples (Fig. 3A, Table 1). Thirty-six connectors and 25 module hubs were detected in the three networks. Only one network hub was detected (Fig. S7), which is affiliated to *Azoarcus* genus. The relative abundances of most keystone taxa were low, except for three keystone nodes with relative abundances greater than 0.5% (Table S5 and Table S6). These three nodes occurred in the 196 N plot and were phylogenetically close to *Flavisolibacter*, *Gp1*, and *Bacillus* genera.

Three modules sensitive to N fertilizer were identified in meta network (Fig. 3B and 3C). In module 1, most species sensitive to excess fertilizer (196N) were clustered together and the cumulative relative abundance of all nodes in this module was increased by 196N. Meanwhile, most indicator species for 0N and 56N were clustered together in module 3 and the cumulative relative abundance of all nodes in this module was decreased by 196N, revealing that the distribution of the sensitive species in modules appeared to be the cause of microbial community changes in Fig. 1.

3.6. Influence of 196N fertilization on microbial functionality

In order to more fully understand the influence of 196N fertilizer on microbial functionality, 0N and 196N samples from plant peak productivity stage were selected for metagenomic analysis. The annotation results from MG-RAST are shown in Fig. 4A. The relative abundances of carbohydrate, coenzyme, vitamin, DNA, phage, and respiratory

metabolism genes were all increased by 196N fertilizer. However, the relative abundances of protein, cell wall, nucleotide, and phosphorus metabolism genes were decreased by 196N fertilizer. Pfam and COG annotation results indicated a significant difference between the 0N and 196N samples, and the addition of excessive fertilizer generally increased the relative abundances of amino acid and carbohydrate metabolism related genes (Fig. S8). KEGG annotation results, however, showed little difference between the two samples, although the relative abundance of dominant carbohydrate metabolism and amino acid metabolism genes were increased by 196N (Fig. 4B). All three annotation results showed that the relative abundance of signal transduction mechanism genes was significantly and dramatically reduced by 196N fertilizer.

Xander software was used to assemble long reads and annotate N cycle related genes (Fig. 5A). PCA results of the *rplB* gene showed that excessive N fertilizer did have a significant effect on the bacterial community structure, which is consistent with 16S rRNA gene analysis (Fig. S9 and Fig. S3A). Archaeal but not bacterial *amoA* genes were detected in both 0N and 196N samples, and the relative abundance of this *amoA* gene increased significantly in the excessive fertilizer treatment, especially for sequences related to *Crenarchaeota* phylum (Fig. 5A), which corresponded to the increased net nitrification rate (Table 2). The *nifH* gene was sporadically observed in a few replicates with relative abundance decreasing under the influence of 196N, corresponding to low N_2 fixation rate (Table 2). The *nirK*, *nirS*, *norB*, and *nosZ* genes are involved in denitrification. The relative abundance of *nirK* gene significantly increased from 657±36 to 888±270 and *nirS* gene decreased from 64±59 to 36±18 with *nirK* gene abundance consistent with field denitrification rate (Table 2). Both are involved in the nitrite reduction step; the *nirK* gene was predominant. The relative abundance of *norB_qNor* was extremely high

compared to *norB_cNor* gene in both 0N and 196N samples. Both of the *norB* genes were not significantly impacted by 196N fertilizer. There was also no significant difference between the two rates for *nosZ* (clade I) and *nosZ*_a2 genes. In general, the denitrifying gene abundance was not obviously changed by 196N fertilizer.

To further confirm the effect of excess N fertilizer on N cycle genes, the N cycle gene information was extracted from the SEED subsystems annotation. As shown in Fig. 5B, the addition of 196N fertilizer significantly decreased relative abundances of some N cycle processes and increased others. Ammonia assimilation, allantoin utilization, N_2 fixation, and cyanate hydrolysis all decreased, while the relative abundances of nitric oxide synthase, amidase, and urea/nitrile hydratase genes increased. Excess N fertilizer did not have a significant impact on the ammonification and denitrification related genes, which corresponded with the Xander result but was inconsistent with the process rates (Table 2).

4. Discussion

We examined the consequences of microbial community structure changes stemming from N fertilizer gradient for the long-term time scale. Similar to previous reports, the application of long-term excess N fertilizer significantly reduces soil pH and dramatically shifts bacterial and fungal community structures, with AMF showing a strong negative response to N fertilizer (Avio et al., 2013; Fierer and Jackson, 2006; Jach-Smith and Jackson, 2018; Jach-Smith and Jackson, 2020; Lauber et al., 2009; Rousk et al., 2009). The analyses of microbial ecological network and functional metagenome, however, gives us a different level of understanding of the influence of N fertilizer on the soil microbiome.

438

439 *4.1. Bacterial communities were more influenced by pH and fungal communities were impacted*
440 *by both pH and fertilizer*

441

442 The copiotrophic hypothesis suggests that oligotrophic bacteria are out-competed by
443 copiotrophic taxa as higher available N allows copiotrophic taxa to use more labile carbon
444 (Fierer et al., 2012a; Ramirez et al., 2012; Zeng et al., 2016). In support we found that N
445 fertilizer increased the relative abundance of copiotrophic groups (*Bacteroidetes* and *Firmicutes*)
446 and decreased oligotrophic groups (*Verrucomicrobia*) (Fig. S4A). At subphylum level, the
447 *Proteobacteria* are typically copiotrophs, and the *Alpha-* and *Gammaproteobacteria* significantly
448 increased at the high fertilizer level but the *Betaproteobacteria* did not (Fig. S4B), which may be
449 due to the acidity. The relative abundance of *Acidobacteria*_Gp1 greatly increased in excess N
450 fertilized soils (Fig. S4B), consistent with its known preference for low pH soil and its recent
451 classification as a copiotroph (Rousk et al., 2010; Yao et al., 2017). In general, the bacterial
452 community diversity and structure were only affected by high fertilizer (196N), not by low
453 fertilizer (56N), which decreased the soil pH as well, but to a lesser degree (Fig.1, S3A, S4(A,
454 B), S5A, Table S1). Many studies show that bacterial community is significantly affected by low
455 pH (Fierer and Jackson, 2006; Lauber et al., 2009; Rousk et al., 2009).

456 The shift in fungal composition occurred at both low and high fertilizer applications at
457 phylum, class and genus level regardless of whether the pH was significantly changed (Fig.
458 S4(C, D), S5B). Therefore, the total fungal community was less responsive to pH than N
459 fertilizer. However, previous global investigation of soil fungi found that several groups were
460 significantly affected by global-scale pH (Tedersoo et al., 2014). A recent study even showed

that soil pH was the most influential factor in determining the total fungal community across three sites of northeast China (Hu et al., 2017). Hence, both pH and fertilizer probably showed interactive effects on these fungal communities, especially for those in 196N plot.

Many surveys have indicated that growing season shows a significant effect on soil bacterial and fungal communities (López-Mondéjar et al., 2015; Voříšková et al., 2014), usually accompanied by significant changes in soil physicochemical properties, root exudates, and/or climate (Inceoğlu et al., 2010; McHugh and Schwartz, 2016; Rasche et al., 2006; Wuest, 2015). We didn't, however, find obvious seasonal changes in the bacterial and fungal community structures, especially with 0N. This might be because most soil chemicals in 0N and 56N plots were stable during the growing season, similar to other studies (Siles and Margesin, 2017), as well as the possible redundancy caused by the increasing carbon input with the growth of switchgrass. Unlike rhizosphere soil chemicals, which can be affected by root exudates and residuals in different growth stage (Shi et al., 2015), bulk soil precluding roots in this study should be less affected by growth stage. Furthermore, stable soil chemicals in the switchgrass field might be attributed to monoculture and annually-harvested biomass, which prevented further nutrients input.

4.2. Microbial co-occurrence network was influenced by long-term excess N fertilizer

After long-term fertilization, the dissimilarity of microbial communities in 196N samples between growing stages was larger than that in 0N and 56N samples (Fig. 2B and Fig. 2D). The higher avgK value and lower HD value of 196N network indicated that the interactions within microbial members in 196N samples were more intense. Both Unifrac distance and network

484 analysis indirectly suggest that 196N samples were more susceptible to external interferences,
485 like plant growth and climate (Table S1). Meta network analysis indicated that species sensitive
486 to N fertilizer were clustered together, suggesting that external disturbances may have a far
487 greater impact on microbial community through targeting sensitive species. In contrast, the
488 dissimilarity of microbial communities in 56N samples between growth stages was smallest (Fig.
489 2B and Fig. 2D). Further, the 56N network showed lower avgK and avgCC, and higher HD and
490 modularity values compared with 196N network, which suggest a sparse interaction among
491 microorganisms in 56N networks and that the microbial populations in 56N treatments were
492 more resistant to environmental changes. Therefore, fertilization rate was an important factor
493 affecting the ecological network relationships.

494 We postulate that long-term addition of excess N fertilizer also reduced the diversity of
495 interactive relationships, which is supported by decreased connections between fungal and
496 bacterial nodes (Table 1). Moreover, the percentage of positive links increased in the 196N
497 network, suggesting that long-term excess N addition might enrich a number of mutualistic
498 microbes (Table 1). As indicated in previous studies, negative links can promote network
499 stability as competition could stabilize co-oscillation in microbial communities (Coyte et al.,
500 2015; Zhou et al., 2020). Previous studies found that addition of straw can decrease negative
501 associations (De Menezes et al., 2015), and covariations are predominantly positive among
502 rhizosphere bacteria where nutrients are usually abundant (Shi et al., 2016). In the 196N plots,
503 nutrients may have alleviated the competition and favored many trophic levels.

504 High abundance is not indicative of a key network role. For instance, the relative
505 abundances of most keystone nodes were very low, i.e. lower than 0.5%, which is consistent with
506 previous findings (Deng et al., 2016; Shi et al., 2016). With the addition of N fertilizer, the

number of the key taxa in the networks increased and their lineages were changed (Table S5 and Table S6). The disappearance of key taxa may cause dissociation of module and network, suggesting that key taxa may play important roles in maintaining network stability (Lu et al., 2013; Olesen et al., 2007; Paine, 1995; Power et al., 1996). The key microbial taxa can change with land use (Lu et al., 2013; Lupatini et al., 2014), where keystone nodes became peripherals with the prolonged potato monoculture and different sets of keystone genera occurred in areas with different land uses at the same site. Similarly, key taxa in this study differed at different N fertilizer levels. It's generally known that more key taxa presented means higher stability of network (Coyte et al., 2015). As shown in Table S5 and S6, the number of key nodes obviously increased with increased N fertilizer level, implying the increased stability of 196N network, which is contrary to the decreased negative links. Single parameter is not enough to predict the stability of network and a series of long-term experiment should be conducted to test it (Yuan et al., 2021). We should be cautious in extending interaction-based ecological theory to interpret network variability and stability (Freilich et al., 2018).

In short, excess N fertilizer may affect the stability of community structure by reducing the interactions between bacteria and fungi but increasing mutualistic relationships among bacteria. In N deficient soils, complex ecological relationships between microorganisms, such as mutualism and competition, may maintain the stability of the community structure. However, the addition of N fertilizer breaks the interdependence of bacteria and fungi and weakens the competition, thus affecting the original ecological network relationships.

4.3. Microbial functionality was significantly influenced by long-term excess N fertilizer

The annotations of metagenomic data based on COG, Pfam, KEGG, and Subsystems databases all showed that long-term excess N fertilization promoted many metabolic processes, especially carbohydrate metabolism, which was similar to a previous, more limited, study in which the soil pH decreased from 6.9 to 5.0 (Fierer et al., 2012a). Sequencing depth in that study was 75000 reads per sample, which is much lower than $4 \sim 5 \times 10^7$ reads per sample in our study. Hence, many possible genes or gene categories were not sufficiently abundant in that previous data set to accurately determine changes in, for example, genes associated with N_2 fixation, lignin degradation, and ammonia oxidation. The much higher sequencing depth in our study not only recovered more genes but allowed assembly of most N cycle genes. Excess N fertilizer also reduced many functional genes, notably signal transduction related genes. A previous study found that genes involved in signal transduction were usually and highly expressed in eutrophic species (Lauro et al., 2009). The addition of high-level N fertilizer should theoretically promote the expression of signal transduction genes, but inhibition occurred, probably because of the influence of low pH and lower bacterial abundance. The decrease in relative abundance of signal transduction-related genes may be associated with the weakened link between bacteria and fungi in the 196N network.

Many studies have indicated that ammonia-oxidizing archaea (AOA) prefer an acidic environment, while ammonia-oxidizing bacteria (AOB) predominate in neutral, alkaline, and N-rich soils (Nicol et al., 2008). In our study, excess N fertilizer acidified the soil, thus creating an environment conducive to growth of AOA. The relative abundance of the N_2 fixation gene (*nifH*) was very low and only detected in some samples, consistent with the lower measured N_2 fixation rate in the fertilized treatment (Roley et al., 2018) (Table 2). N_2 fixation requires high energy and its rates typically decrease as soil N becomes abundant (Gelfand et al., 2015). In contrast, both

553 Xander and SEED subsystem annotations indicated that the denitrification potential was not
554 significantly impacted by long-term excess N fertilizer, except *nirK* gene. However, the
555 denitrification rate was increased in the 196N treatment (Table 2). Similarity, some studies found
556 that the addition of urea increased the abundance of *nirK* and *nirS* genes or N_2O production rate
557 (Wang et al., 2015; Zhong et al., 2017). However, other studies show that the addition of high-
558 concentration of N fertilizers reduced the abundance of *nirK* and *nirS* or *nosZ* genes (Kastl et al.,
559 2014; Tang et al., 2016). In general, the denitrification process is affected by many factors such
560 as available nitrate, pH, organic carbon, oxygen availability, moisture, soil texture, temperature,
561 and plant species (Faulwetter et al., 2009; Wallenstein et al., 2006). At peak productivity, higher
562 nitrate content in 196N soil potentially increased denitrification rate as available nitrate
563 increased. Nitrate is a common proximal control on denitrification rate. But the low pH in 196N
564 soil may impact denitrification gene abundance by influencing denitrifying population and soil
565 organic carbon (Šimek et al., 2002). Hence, in our study, and probably in many cases, the
566 denitrifying enzyme capacities measured by gene amounts exceed the actual rates, and hence a
567 direct gene-activity relationship is not expected. This is more likely the case with denitrification
568 than other nitrogen cycle processes, as seen here, because others are less dynamically controlled
569 by environmental conditions.
570
571 **5. Conclusions**
572
573 As we hypothesized, bacterial and fungal communities were significantly changed by
574 long-term excess N fertilizer because of high nutrient and low pH. Unexpectedly, soil microbial
575 community structures didn't change during the growing season, consistent with the lack of

seasonal changes in soil physicochemical properties. However, microbial communities became more susceptible to the external environment under the influence of long-term excess N fertilizer. Excess N fertilizer also significantly changed microbial co-occurrence relationships with decreased bacteria-fungi interactions and increased positive connectivity and number of keystone taxa. Moreover, excess N fertilizer changed bacterial function: it was beneficial to AOA, but adverse to N_2 fixation, and no significant change of denitrifying gene abundance. Our results demonstrated that excess N fertilizer not only changes microbial community composition and metabolic potential, it alters microbial relationships, with potential consequences for stability.

Acknowledgements

Support for this research was provided by the U.S. Department of Energy, Office of Science, Office of Biological and Environmental Research (Awards DE-SC0018409 and DE-FC02-07ER64494), by the National Science Foundation Long-term Ecological Research Program (DEB 1637653) at Kellogg Biological Station, and by Michigan State University AgBioResearch. The sequencing was performed by DOE's Joint Genome Institute, a DOE Office of Science User Facility, and was supported by the Office of Science of the U.S. Department of Energy under Contract No. DE-AC02-05CH11231.

References

598 Apprill, A., Mcnally, S., Parsons, R., Weber, L., 2015. Minor revision to V4 region SSU rRNA
599 806R gene primer greatly increases detection of SAR11 bacterioplankton. Aquatic
600 Microbial Ecology 75, 129–137.
601 Aulakh, M.S., Wassmann, R., Bueno, C., Kreuzwieser, J., Rennenberg, H., 2001.
602 Characterization of root exudates at different growth stages of ten rice (*Oryza sativa* L.)
603 cultivars. Plant Biology 3, 139–148.
604 Avio, L., Castaldini, M., Fabiani, A., Bedini, S., Sbrana, C., Turrini, A., Giovannetti, M., 2013.
605 Impact of nitrogen fertilization and soil tillage on arbuscular mycorrhizal fungal
606 communities in a Mediterranean agroecosystem. Soil Biology and Biochemistry 67, 285–
607 294.
608 Badri, D. V., Vivanco, J.M., 2009. Regulation and function of root exudates. Plant, Cell &
609 Environment 32, 666–681.
610 Banerjee, S., Kirkby, C.A., Schmutter, D., Bissett, A., Kirkegaard, J.A., Richardson, A.E., 2016.
611 Network analysis reveals functional redundancy and keystone taxa amongst bacterial and
612 fungal communities during organic matter decomposition in an arable soil. Soil Biology and
613 Biochemistry 97, 188–198.
614 Bastian, M., Heymann, S., Jacomy, M., 2009. Gephi: an open source software for exploring and
615 manipulating networks. International AAAI Conference on Weblogs and Social Media.
616 Bengtsson-Palme, J., Ryberg, M., Hartmann, M., Branco, S., Wang, Z., Godhe, A., De Wit, P.,
617 Sánchez-García, M., Ebersberger, I., de Sousa, F., Amend, A., Jumpponen, A., Unterseher,
618 M., Kristiansson, E., Abarenkov, K., Bertrand, Y.J.K., Sanli, K., Eriksson, K.M., Vik, U.,
619 Veldre, V., Nilsson, R.H., 2013. Improved software detection and extraction of ITS1 and

620 ITS2 from ribosomal ITS sequences of fungi and other eukaryotes for analysis of
621 environmental sequencing data. Methods in Ecology and Evolution 4, 914–919.
622 Benoit, I., van den Esker, M.H., Patyshakuliyeva, A., Mattern, D.J., Blei, F., Zhou, M.,
623 Dijksterhuis, J., Brakhage, A.A., Kuipers, O.P., de Vries, R.P., Kovács, Á.T., 2015. *Bacillus*
624 *subtilis* attachment to *Aspergillus niger* hyphae results in mutually altered metabolism.
625 Environmental Microbiology 17, 2099–2113.
626 Boer, W. de, Folman, L.B., Summerbell, R.C., Boddy, L., 2005. Living in a fungal world: impact
627 of fungi on soil bacterial niche development. FEMS Microbiology Reviews 29, 795–811.
628 Bolger, A.M., Lohse, M., Usadel, B., 2014. Trimmomatic: A flexible trimmer for Illumina
629 sequence data. Bioinformatics 30, 2114–2120.
630 Bushnell, B., 2015. BBMap (version 35.14) [Software]. Available at
631 Https://Sourceforge.Net/Projects/Bbmap/.
632 Csardi, G., Nepusz, T., 2006. The igraph software package for complex network research,
633 InterJournal, Complex Systems. 1695. http://igraph.org.
634 Chemidlin Prevost-Boure, N., Christen, R., Dequiedt, S., Mougel, C., Lelievre, M., Jolivet, C.,
635 Shahbazkia, H.R., Guillou, L., Arrouays, D., Ranjard, L., 2011. Validation and application
636 of a PCR primer set to quantify fungal communities in the soil environment by real-time
637 quantitative PCR. PLoS ONE 6, 1–13.
638 Cole, J.R., Wang, Q., Fish, J.A., Chai, B., McGarrell, D.M., Sun, Y., Brown, C.T., Porras-Alfaro,
639 A., Kuske, C.R., Tiedje, J.M., 2014. Ribosomal Database Project: data and tools for high
640 throughput rRNA analysis. Nucleic Acids Research 42, D633–D642.
641 Coyte, K.Z., Schluter, J., Foster, K.R., 2015. The ecology of the microbiome: Networks,
642 competition, and stability. Science 350, 663–666.

643 De Menezes, A.B., Prendergast-Miller, M.T., Richardson, A.E., Toscas, P., Farrell, M.,
644 Macdonald, L.M., Baker, G., Wark, T., Thrall, P.H., 2015. Network analysis reveals that
645 bacteria and fungi form modules that correlate independently with soil parameters.
646 Environmental Microbiology 17, 2677–2689.
647 DeAngelis, M.M., Wang, D.G., Hawkins, T.L., 1995. Solid-phase reversible immobilization for
648 the isolation of PCR products. Nucleic Acids Research 23, 4742–4743.
649 De Cáceres, M., Legendre, P., Moretti, M., 2010. Improving indicator species analysis by
650 combining groups of sites. Oikos 119, 1674–84.
651 Deng, Y., Jiang, Y.-H., Yang, Y., He, Z., Luo, F., Zhou, J., 2012. Molecular ecological network
652 analyses. BMC Bioinformatics 13, 113.
653 Deng, Y., Zhang, P., Qin, Y., Tu, Q., Yang, Y., He, Z., Schadt, C.W., Zhou, J., 2016. Network
654 succession reveals the importance of competition in response to emulsified vegetable oil
655 amendment for uranium bioremediation. Environmental Microbiology 18, 205–218.
656 Dixon, P., 2003. VEGAN, a package of R functions for community ecology. Journal of
657 Vegetation Science 14, 927–930.
658 Eddy, S.R., 2011. Accelerated Profile HMM Searches. PLoS Computational Biology 7,
659 e1002195.
660 Edgar, R.C., 2013. UPARSE: Highly accurate OTU sequences from microbial amplicon reads.
661 Nature Methods 10, 996–998.
662 Edgar, R.C., 2010. Search and clustering orders of magnitude faster than BLAST. Bioinformatics
663 26, 2460–2461.
664 Edgar, R.C., Haas, B.J., Clemente, J.C., Quince, C., Knight, R., 2011. UCHIME improves
665 sensitivity and speed of chimera detection. Bioinformatics 27, 2194–2200.

666 Faulwetter, J.L., Gagnon, V., Sundberg, C., Chazarenc, F., Burr, M.D., Brisson, J., Camper,
667 A.K., Stein, O.R., 2009. Microbial processes influencing performance of treatment
668 wetlands: A review. Ecological Engineering 35, 987–1004.
669 Fierer, N., Jackson, R.B., 2006. The diversity and biogeography of soil bacterial communities.
670 Proceedings of the National Academy of Sciences of the United States of America 103,
671 626–631.
672 Fierer, N., Lauber, C.L., Ramirez, K.S., Zaneveld, J., Bradford, M.A., Knight, R., 2012a.
673 Comparative metagenomic, phylogenetic and physiological analyses of soil microbial
674 communities across nitrogen gradients. ISME Journal 6, 1007–1017.
675 Fierer, N., Leff, J.W., Adams, B.J., Nielsen, U.N., Bates, S.T., Lauber, C.L., Owens, S., Gilbert,
676 J.A., Wall, D.H., Caporaso, J.G., 2012b. Cross-biome metagenomic analyses of soil
677 microbial communities and their functional attributes. Proceedings of the National
678 Academy of Sciences 109, 21390–21395.
679 Fike, J.H., Pease, J.W., Owens, V.N., Farris, R.L., Hansen, J.L., Heaton, E.A., Hong, C.O.,
680 Mayton, H.S., Mitchell, R.B., Viands, D.R., 2017. Switchgrass nitrogen response and
681 estimated production costs on diverse sites. GCB Bioenergy 9, 1526–1542.
682 Finn, R.D., Coggill, P., Eberhardt, R.Y., Eddy, S.R., Mistry, J., Mitchell, A.L., Potter, S.C.,
683 Punta, M., Qureshi, M., Sangrador-Vegas, A., Salazar, G.A., Tate, J., Bateman, A., 2016.
684 The Pfam protein families database: Towards a more sustainable future. Nucleic Acids
685 Research 44, D279–D285.
686 Freilich, M.A., Wieters, E., Broitman, B.R., Marquet, P.A., Navarrete, S.A., 2018. Species co-
687 occurrence networks: Can they reveal trophic and non-trophic interactions in ecological
688 communities? Ecology 99, 690–699.

689 Gallo, M., Amonette, R., Lauber, C., Sinsabaugh, R.L., Zak, D.R., 2004. Microbial community
690 structure and oxidative enzyme activity in nitrogen-amended north temperate forest soils.
691 Microbial Ecology 48, 218–229.
692 Gelfand, I., Robertson, G.P., 2015. A reassessment of the contribution of soybean biological
693 nitrogen fixation to reactive N in the environment. Biogeochemistry 123, 175–84.
694 Geisseler, D., Scow, K.M., 2014. Long-term effects of mineral fertilizers on soil microorganisms
695 - A review. Soil Biology and Biochemistry 75, 54–63.
696 Hu, X., Liu, J., Wei, D., Zhu, P., Cui, X., Zhou, B., Chen, X., Jin, J., Liu, X., Wang, G., 2017.
697 Effects of over 30-year of different fertilization regimes on fungal community compositions
698 in the black soils of northeast China. Agriculture, Ecosystems and Environment 248, 113–
699 122.
700 Ihrmark, K., Bödeker, I.T.M., Cruz-Martinez, K., Friberg, H., Kubartova, A., Schenck, J., Strid,
701 Y., Stenlid, J., Brandström-Durling, M., Clemmensen, K.E., Lindahl, B.D., 2012. New
702 primers to amplify the fungal ITS2 region - evaluation by 454-sequencing of artificial and
703 natural communities. FEMS Microbiology Ecology 82, 666–677.
704 Inceoğlu, Ö., Salles, J.F., Van Overbeek, L., Van Elsas, J.D., 2010. Effects of plant genotype and
705 growth stage on the betaproteobacterial communities associated with different potato
706 cultivars in two fields. Applied and Environmental Microbiology 76, 3675–3684.
707 Jach-Smith, L.C., Jackson, R.D., 2018. N addition undermines N supplied by arbuscular
708 mycorrhizal fungi to native perennial grasses. Soil Biology and Biochemistry 116, 148–157.
709 Jach-Smith, L.C., Jackson, R.D., 2020. Inorganic N addition replaces N supplied to switchgrass
710 (*Panicum virgatum*) by arbuscular mycorrhizal fungi. Ecological Applications 30.

711 Kanehisa, M., Sato, Y., Kawashima, M., Furumichi, M., Tanabe, M., 2016. KEGG as a reference
712 resource for gene and protein annotation. Nucleic Acids Research 44, D457–D462.
713 Kastl, E.M., Schloter-Hai, B., Buegger, F., Schloter, M., 2014. Impact of fertilization on the
714 abundance of nitrifiers and denitrifiers at the root–soil interface of plants with different
715 uptake strategies for nitrogen. Biology and Fertility of Soils 51, 57–64.
716 Lauber, C.L., Hamady, M., Knight, R., Fierer, N., 2009. Soil pH as a predictor of soil bacterial
717 community structure at the continental scale: a pyrosequencing-based assessment. Applied
718 and Environmental Microbiology 75, 5111–5120.
719 Lauro, F.M., McDougald, D., Thomas, T., Williams, T.J., Egan, S., Rice, S., DeMaere, M.Z.,
720 Ting, L., Ertan, H., Johnson, J., Ferriera, S., Lapidus, A., Anderson, I., Kyrpides, N., Munk,
721 A.C., Detter, C., Han, C.S., Brown, M. V., Robb, F.T., Kjelleberg, S., Cavicchioli, R., 2009.
722 The genomic basis of trophic strategy in marine bacteria. Proceedings of the National
723 Academy of Sciences 106, 15527–15533.
724 Lees, J.G., Lee, D., Studer, R.A., Dawson, N.L., Sillitoe, I., Das, S., Yeats, C., Dessailly, B.H.,
725 Rentzsch, R., Orengo, C.A., Hunter, S., Corbett, M., Denise, H., Fraser, M., Gonzalez-
726 Beltran, A., Hunter, C., Jones, P., Leinonen, R., McAnulla, C., Maguire, E., Maslen, J.,
727 Mitchell, A., Nuka, G., Oisel, A., Pesseat, S., Radhakrishnan, R., Rocca-Serra, P.,
728 Scheremetjew, M., Sterk, P., Vaughan, D., Cochrane, G., Field, D., Sansone, S.-A., Hyatt,
729 D., LoCascio, P.F., Hauser, L.J., Uberbacher, E.C., Katoh, K., Standley, D.M., Meyer, F.,
730 Paarmann, D., D'Souza, M., Olson, R., Glass, E.M., Kubal, M., Paczian, T., Rodriguez, A.,
731 Stevens, R., Wilke, A., Wilkening, J., Edwards, R.A., Peng, Y., Leung, H.C.M., Yiu, S.M.,
732 Chin, F.Y.L., Rice, P., Longden, I., Bleasby, A., 2014. The metagenomics RAST server - a

733 public resource for the automatic phylogenetic and functional analysis of metagenomes.
734 Bioinformatics (Oxford, England) 28, 772–780.
735 Leff, J.W., Jones, S.E., Prober, S.M., Barberán, A., Borer, E.T., Firn, J.L., Harpole, W.S.,
736 Hobbie, S.E., Hofmockel, K.S., Knops, J.M.H., McCulley, R.L., La Pierre, K., Risch, A.C.,
737 Seabloom, E.W., Schütz, M., Steenbock, C., Stevens, C.J., Fierer, N., 2015. Consistent
738 responses of soil microbial communities to elevated nutrient inputs in grasslands across the
739 globe. Proceedings of the National Academy of Sciences 112, 10967–10972.
740 Li, D., Liu, C.M., Luo, R., Sadakane, K., Lam, T.W., 2015. MEGAHIT: An ultra-fast single-
741 node solution for large and complex metagenomics assembly via succinct de Bruijn graph.
742 Bioinformatics 31, 1674–1676.
743 López-Mondéjar, R., Voříšková, J., Větrovský, T., Baldrian, P., 2015. The bacterial community
744 inhabiting temperate deciduous forests is vertically stratified and undergoes seasonal
745 dynamics. Soil Biology and Biochemistry 87, 43–50.
746 Lu, L., Yin, S., Liu, X., Zhang, W., Gu, T., Shen, Q., Qiu, H., 2013. Fungal networks in yield-
747 invigorating and -debilitating soils induced by prolonged potato monoculture. Soil Biology
748 and Biochemistry 65, 186–194.
749 Lucas García, J.A., Barbas, C., Probanza, A., Barrientos, M.L., Gutierrez Mañero, F.J., 2001.
750 Low molecular weight organic acids and fatty acids in root exudates of two Lupinus
751 cultivars at flowering and fruiting stages. Phytochemical Analysis 12, 305–311.
752 Lupatini, M., Suleiman, A.K.A., Jacques, R.J.S., Antoniolli, Z.I., de Siqueira Ferreira, A.,
753 Kuramae, E.E., Roesch, L.F.W., 2014. Network topology reveals high connectance levels
754 and few key microbial genera within soils. Frontiers in Environmental Science 2.

Ma, B., Wang, H., Dsouza, M., Lou, J., He, Y., Dai, Z., Brookes, P.C., Xu, J., Gilbert, J.A., 2016. Geographic patterns of co-occurrence network topological features for soil microbiota at continental scale in eastern China. ISME Journal 10, 1891–1901.

McHugh, T.A., Schwartz, E., 2016. A watering manipulation in a semiarid grassland induced changes in fungal but not bacterial community composition. Pedobiologia 59, 121–127.

Meier, C.L., Bowman, W.D., 2008. Links between plant litter chemistry, species diversity, and below-ground ecosystem function. Proceedings of the National Academy of Sciences 105, 19780–19785.

Monti, A., 2012. Switchgrass, Green Energy and Technology, Green Energy and Technology. Springer London, London.

Nelson, M.B., Martiny, A.C., Martiny, J.B.H., 2016. Global biogeography of microbial nitrogen-cycling traits in soil. Proceedings of the National Academy of Sciences 113, 8033–8040.

Nicol, G.W., Leininger, S., Schleper, C., Prosser, J.I., 2008. The influence of soil pH on the diversity, abundance and transcriptional activity of ammonia oxidizing archaea and bacteria. Environmental Microbiology 10, 2966–2978.

Olesen, J.M., Bascompte, J., Dupont, Y.L., Jordano, P., 2007. The modularity of pollination networks. Proceedings of the National Academy of Sciences 104, 19891–19896.

Orellana, L.H., Chee-Sanford, J.C., Sanford, R.A., Löffler, F.E., Konstantinidis, K.T., 2017. Year-round shotgun metagenomes reveal stable microbial communities in agricultural soils and novel ammonia oxidizers responding to fertilization. Applied and Environmental Microbiology 84, e01646-17.

Paine, R.T., 1995. A Conversation on refining the concept of keystone species. Conservation Biology 9, 962–964.

778 Parrish, D.J., Fike, J.H., 2005. The biology and agronomy of switchgrass for biofuels. Critical
779 Reviews in Plant Sciences 24, 423–459.
780 Paungfoo-Lonhienne, C., Yeoh, Y.K., Kasinadhuni, N.R.P., Lonhienne, T.G.A., Robinson, N.,
781 Hugenholtz, P., Ragan, M.A., Schmidt, S., 2015. Nitrogen fertilizer dose alters fungal
782 communities in sugarcane soil and rhizosphere. Scientific Reports 5, 8678.
783 Power, M.E., Tilman, D., Estes, J.A., Menge, B.A., Bond, W.J., Mills, L.S., Daily, G., Castilla,
784 J.C., Lubchenco, J., Paine, R.T., 1996. Challenges in the quest for keystones. BioScience
785 46, 609–620.
786 Ramirez, K.S., Craine, J.M., Fierer, N., 2012. Consistent effects of nitrogen amendments on soil
787 microbial communities and processes across biomes. Global Change Biology 18, 1918–
788 1927.
789 Rasche, F., Hödl, V., Poll, C., Kandeler, E., Gerzabek, M.H., Van Elsas, J.D., Sessitsch, A.,
790 2006. Rhizosphere bacteria affected by transgenic potatoes with antibacterial activities
791 compared with the effects of soil, wild-type potatoes, vegetation stage and pathogen
792 exposure. FEMS Microbiology Ecology 56, 219–235.
793 Robertson, G.P., Wedin, D., Groffman, P.M., Blair, J.M., Holland, E.A., Nadelhoffer, K., Harris,
794 D., 1999. Soil carbon and nitrogen availability: Nitrogen mineralization, nitrification, and
795 soil respiration potentials. In G.P. Robertson, D.C. Coleman, C.S. Bledsoe, & P. Sollins
796 (Eds.), Standard Soil Methods for Long-Term Ecological Research. New York: Oxford
797 University Press.
798 Robinson, M.D., McCarthy, D.J., Smyth, G.K., 2010. edgeR: a bioconductor package for
799 differential expression analysis of digital gene expression data. Bioinformatics 26, 139–40.

800 Roley, S.S., Duncan, D.S., Liang, D., Garoutte, A., Jackson, R.D., Tiedje, J.M., Robertson, G.P.,
801 2018. Associative nitrogen fixation (ANF) in switchgrass (Panicum virgatum) across a
802 nitrogen input gradient. PloS One 13, e0197320.
803 Rousk, J., Bååth, E., Brookes, P.C., Lauber, C.L., Lozupone, C., Caporaso, J.G., Knight, R.,
804 Fierer, N., 2010. Soil bacterial and fungal communities across a pH gradient in an arable
805 soil. Isme J. 4, 1340–1351.
806 Rousk, J., Brookes, P.C., Bååth, E., 2009. Contrasting soil pH effects on fungal and bacterial
807 growth suggest functional redundancy in carbon mineralization. Applied and Environmental
808 Microbiology 75, 1589–1596.
809 Ruan, L., Bhardwaj, A.K., Hamilton, S.K., Robertson, G.P., 2016. Nitrogen fertilization
810 challenges the climate benefit of cellulosic biofuels. Environmental Research Letters 11,
811 064007.
812 Sanford, G.R., Oates, L.G., Jasrotia, P., Thelen, K.D., Robertson, G.P., Jackson, R.D., 2016.
813 Comparative productivity of alternative cellulosic bioenergy cropping systems in the North
814 Central USA. Agriculture, Ecosystems & Environment 216, 344–355.
815 Shi, S., Nuccio, E., Herman, D.J., Rijkers, R., Estera, K., Li, J., da Rocha, U.N., He, Z., Pett-
816 Ridge, J., Brodie, E.L., Zhou, J., Firestone, M., 2015. Successional trajectories of
817 rhizosphere bacterial communities over consecutive seasons. mBio 6, e00746-15.
818 Shi, S., Nuccio, E.E., Shi, Z.J., He, Z., Zhou, J., Firestone, M.K., 2016. The interconnected
819 rhizosphere: High network complexity dominates rhizosphere assemblages. Ecology Letters
820 19, 926–936.

Siles, J.A., Margesin, R., 2017. Seasonal soil microbial responses are limited to changes in functionality at two Alpine forest sites differing in altitude and vegetation. Scientific Reports 7, 2204.

Šimek, M., Cooper, J.E., 2002. The influence of soil pH on denitrification: progress towards the understanding of this interaction over the last 50 years. European Journal of Soil Science 53, 345–354.

Tang, Y., Zhang, X., Li, D., Wang, H., Chen, F., Fu, X., Fang, X., Sun, X., Yu, G., 2016. Impacts of nitrogen and phosphorus additions on the abundance and community structure of ammonia oxidizers and denitrifying bacteria in Chinese fir plantations. Soil Biology and Biochemistry 103, 284–293.

Tatusov, R.L., Fedorova, N.D., Jackson, J.D., Jacobs, A.R., Kiryutin, B., Koonin, E. V., Krylov, D.M., Mazumder, R., Smirnov, S., Nikolskaya, A.N., Rao, B.S., Mekhedov, S.L., Sverlov, A. V., Vasudevan, S., Wolf, Y.I., Yin, J.J., Natale, D.A., 2003. The COG database: An updated vesion includes eukaryotes. BMC Bioinformatics 4.

Tedersoo, L., Bahram, M., Polme, S., Koljalg, U., Yorou, N.S., Wijesundera, R., Ruiz, L. V., Vasco-Palacios, A.M., Thu, P.Q., Suija, A., Smith, M.E., Sharp, C., Saluveer, E., Saitta, A., Rosas, M., Riit, T., Ratkowsky, D., Pritsch, K., Poldmaa, K., Piepenbring, M., Phosri, C., Peterson, M., Parts, K., Partel, K., Otsing, E., Nouhra, E., Njouonkou, A.L., Nilsson, R.H., Morgado, L.N., Mayor, J., May, T.W., Majuakim, L., Lodge, D.J., Lee, S.S., Larsson, K.-H., Kohout, P., Hosaka, K., Hiiesalu, I., Henkel, T.W., Harend, H., Guo, L. -d., Greslebin, A., Grelet, G., Geml, J., Gates, G., Dunstan, W., Dunk, C., Drenkhan, R., Dearnaley, J., De Kesel, A., Dang, T., Chen, X., Buegger, F., Brearley, F.Q., Bonito, G., Anslan, S., Abell, S.,

Abarenkov, K., 2014. Global diversity and geography of soil fungi. Science 346, 1256688–1256688.

Voříšková, J., Brabcová, V., Cajthaml, T., Baldrian, P., 2014. Seasonal dynamics of fungal communities in a temperate oak forest soil. New Phytologist 201, 269–278.

Wallenstein, M.D., Myrold, D.D., Firestone, M., Voytek, M., 2006. Environmental controls on denitrifying communities and denitrification rates: Insights from molecular methods. Ecological Applications 16, 2143-2152.

Wang, N., Ding, L.-J., Xu, H.-J., Li, H.-B., Su, J.-Q., Zhu, Y.-G., 2015. Variability in responses of bacterial communities and nitrogen oxide emission to urea fertilization among various flooded paddy soils. FEMS Microbiology Ecology 91.

Wang, Q., Fish, J.A., Gilman, M., Sun, Y., Brown, C.T., Tiedje, J.M., Cole, J.R., 2015. Xander: employing a novel method for efficient gene-targeted metagenomic assembly. Microbiome 3, 32.

Wang, Q., Garrity, G.M., Tiedje, J.M., Cole, J.R., 2007. Naïve Bayesian classifier for rapid assignment of rRNA sequences into the new bacterial taxonomy. Applied and Environmental Microbiology 73, 5261–5267.

Wang, S., Sanford, G.R., Robertson, P.G., Jackson, R.D., Thelen, K.D., 2019. Perennial bioenergy crop yield and quality response to nitrogen fertilization. BioEnergy Research 13, 157–166.

Warmink, J.A., Nazir, R., Van Elsas, J.D., 2009. Universal and species-specific bacterial "fungiphiles" in the mycospheres of different basidiomycetous fungi. Environmental Microbiology 11, 300–312.

Wickham, H., 2009. ggplot2, Media. Springer New York, New York, NY.

866 Wuest, S.B., 2015. Seasonal variation in soil bulk density, organic nitrogen, available
867 phosphorus, and pH. Soil Science Society of America Journal 79, 1188–1197.
868 Yan, G., Xing, Y., Xu, L., Wang, J., Dong, X., Shan, W., Guo, L., Wang, Q., 2017. Effects of
869 different nitrogen additions on soil microbial communities in different seasons in a boreal
870 forest. Ecosphere 8, e01879.
871 Yao, F., Yang, S., Wang, Z., Wang, Xue, Ye, J., Wang, Xugao, DeBruyn, J.M., Feng, X., Jiang,
872 Y., Li, H., 2017. Microbial taxa distribution is associated with ecological trophic cascades
873 along an elevation gradient. Frontiers in Microbiology 8.
874 Yuan, M.M., Guo, X., Wu, L., Zhang, Y., Xiao, N., Ning, D., Shi, Z., Zhou, X., Wu, L., Yang,
875 Y., Tiedje, J.M., Zhou, J., 2021. Climate warming enhances microbial network complexity
876 and stability. Nature Climate Change 11, 343–348.
877 Zeng, J., Liu, X., Song, L., Lin, X., Zhang, H., Shen, C., Chu, H., 2016. Nitrogen fertilization
878 directly affects soil bacterial diversity and indirectly affects bacterial community
879 composition. Soil Biology and Biochemistry 92, 41–49.
880 Zhong, Y., Wang, X., Yang, J., Zhao, X., 2017. Tracing the fate of nitrogen with 15N isotope
881 considering suitable fertilizer rate related to yield and environment impacts in paddy field.
882 Paddy Water Environviroment 15, 943–949.
883 Zhou, H., Gao, Y., Jia, X., Wang, M., Ding, J., Cheng, L., Bao, F., Wu, B., 2020. Network
884 analysis reveals the strengthening of microbial interaction in biological soil crust
885 development in the Mu Us Sandy Land, northwestern China. Soil Biology and Biochemistry
886 144, 107782.
887 Zhou, J., Deng, Y., Luo, F., He, Z., Yang, Y., 2011. Phylogenetic molecular ecological network
888 of soil microbial communities in response to elevated CO_2. MBio 2, e00122-11

889

890 **Table 1** Topological properties of the empirical phylogenetic molecular ecological networks

891 (pMENs) across the N fertilizer gradient in comparison to the random networks

	Network Indexes	0N	56N	196N
Empirical networks	Similarity threshold	0.880	0.880	0.880
	R square of power-law	0.962	0.952	0.838
	Average connectivity (avgK)	2.671	2.976	11.849
	Average clustering coefficient (avgCC)	0.135	0.161	0.301
	Harmonic geodesic distance (HD)	5.796	5.833	3.106
	Density (D)	0.004	0.005	0.02
	Modularity (no. of modules)	0.807 (130)	0.757 (105)	0.337 (71)
	Bacterial nodes	515 (79.2%)	535 (85.6%)	530 (88.6%)
	Fungal nodes	135 (20.8%)	90 (14.4%)	68 (11.4%)
	Total nodes (Network size)	650	625	598
	Links within bacterial nodes	629 (72.5%)	751 (80.7%)	3355 (94.7%)
	Links within fungal nodes	68 (7.8%)	22 (2.4%)	28 (0.8%)
	Links between bacterial and fungal nodes	171 (19.7%)	157 (16.9%)	160 (4.5%)
	Negative links	243 (28.0%)	254 (27.3%)	429 (12.1%)
	Positive links	625 (72.0%)	676 (72.7%)	3114 (87.9%)
	Total links	868	930	3543
Random networks	Average clustering coefficient (avgCC)	0.007 ± 0.003	0.011 ± 0.004	0.127 ± 0.006
	Harmonic geodesic distance (HD)	4.584 ± 0.059	4.249 ± 0.041	2.710 ± 0.015
	Modularity(fast_greedy)	0.678 ± 0.007	0.625 ± 0.005	0.207 ± 0.004

892

893

894 **Table 2** N cycle related process rates and corresponding gene abundances for 0N and 196N
895 samples from peak productivity stage. Rate data was from reference (Roley et al., 2018) except
896 denitrification and N_2O production, which are unpublished.

N processes (μg N/g soil/d)	N_2 fixation rate	Net nitrification rate	Net ammonification	Field denitrification rate	Field N_2O production rate
KBS3_0N	1.04 ± 0.37	0.35 ± 0.19	-0.24 ± 0.10	0.0010 ± 0.0009	0.0002 ± 0.0001
KBS3_196N	0.66 ± 0.30	0.64 ± 0.13	-0.13 ± 0.05	0.0021 ± 0.0011	0.0011 ± 0.0008
N cycle gene abundance	*nifH* abundance per 10000 *rplB*	*amoA* abundance per 10000 *rplB*	Ammonification related gene (%)	*nirK* abundance per 10000 *rplB*	*norB* abundance per 10000 *rplB*
KBS3_0N	12.0 ± 10.5	73.7 ± 36.5	0.334 ± 0.019	656.7 ± 35.9	2069.6 ± 446.5
KBS3_196N	6.5 ± 7.8	272.6 ± 65.6	0.303 ± 0.006	888.4 ± 270.1	1664.5 ± 357.0

897

Figure captions

Fig. 1. Beta diversities of bacterial communities (A) and fungal communities (B) for all samples. Principal coordinates analysis (PCoA) based on weighted UniFrac distance was adopted to analyze beta diversity. 0N, 56N, and 196N represent different N fertilizer rates. Pre, Post, Peak and Sene represent four growth stages, which are pre-fertilization, post-fertilization, peak productivity and senescence, respectively. $*P < 0.05$, $**P < 0.01$, $***P < 0.001$: the microbial communities were significantly different among treatments.

Fig. 2. UniFrac distance between N fertilizer rates (A, C) and growth stages (B, D) for bacterial community (A, B) and fungal community (C, D). 0N, 56N and 196N represent different N fertilizer rates. Pre, Post, Peak and Sene represent four growth stages, which are pre-fertilization, post-fertilization, peak productivity and senescence, respectively. Significance: $*P < 0.05$, $**P < 0.01$, $***P < 0.001$.

Fig. 3. Co-occurrence networks of bacteria and fungi for three N fertilizer rates (A), meta co-occurrence pattern of bacteria and fungi for all samples (B), and cumulative relative abundance (as counts per million) of all OTUs in N sensitive modules in meta network (C). The gray OTUs in Fig. B are insensitive to N fertilizer. The colorful OTUs in Fig. B indicate sensitive microbes to different N fertilizer rates.

Fig. 4. Relative abundance of grouped function genes annotated based on Subsystems database (A) and KEGG database (B) in 0N and 196N samples from peak productivity stage. Significance: **P* < 0.05, ***P* < 0.01, ****P* < 0.001.

Fig. 5. Relative abundance of N cycle genes per 10,000 *rplB* annotated by Xander software (A) and relative abundance of N metabolism related gene groups annotated by Subsystems database (B) in 0N and 196N fertilizer samples from peak productivity stage. Asterisk indicates significant difference between 0N and 196N.

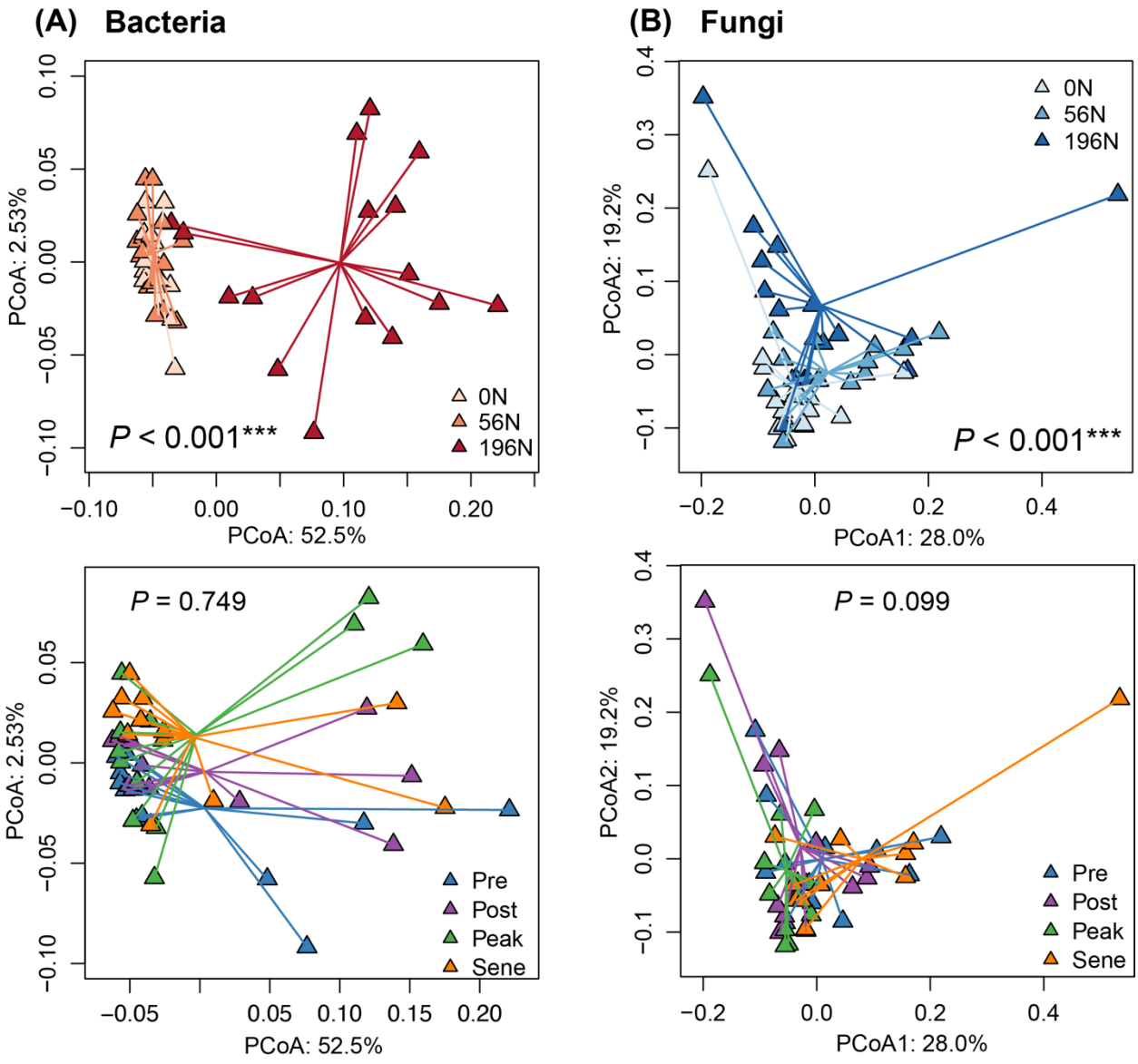
(A) Bacteria
(B) Fungi
PCoA: 2.53%
PCoA: 52.5%
PCoA2: 19.2%
PCoA1: 28.0%
0N
56N
196N
P < 0.001***
P = 0.749
P = 0.099
Pre
Post
Peak
Sene

927

928 **Fig. 1**

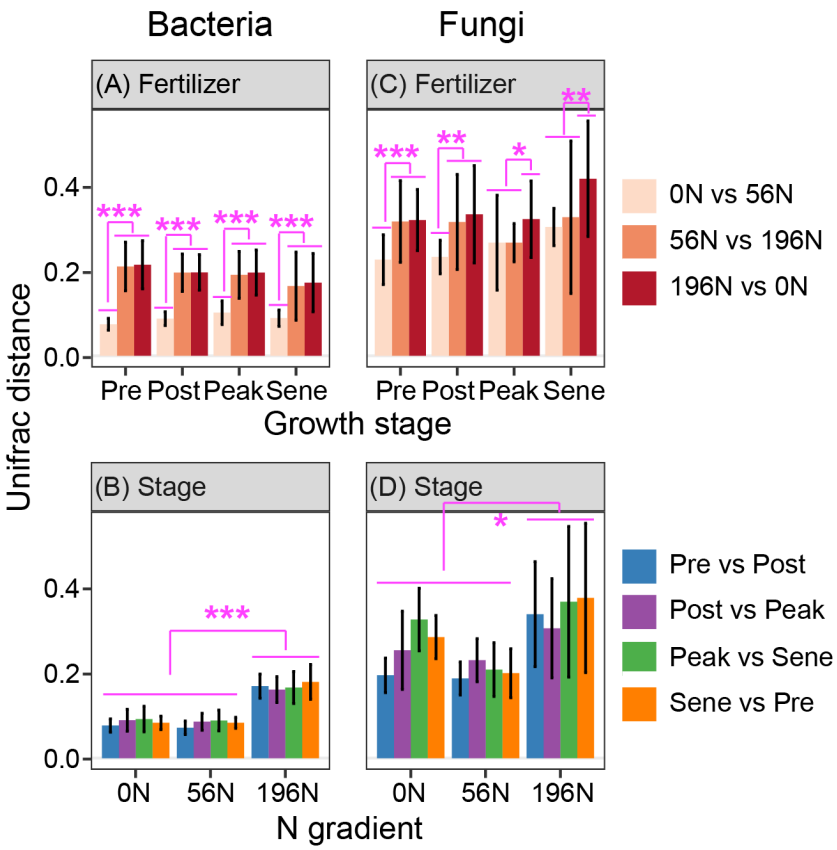
Bacteria
Fungi
(A) Fertilizer
(C) Fertilizer
(B) Stage
(D) Stage
Unifrac distance
0.0
0.2
0.4
Pre Post Peak Sene
Growth stage
0N
56N
196N
N gradient
0N vs 56N
56N vs 196N
196N vs 0N
Pre vs Post
Post vs Peak
Peak vs Sene
Sene vs Pre

Fig. 2

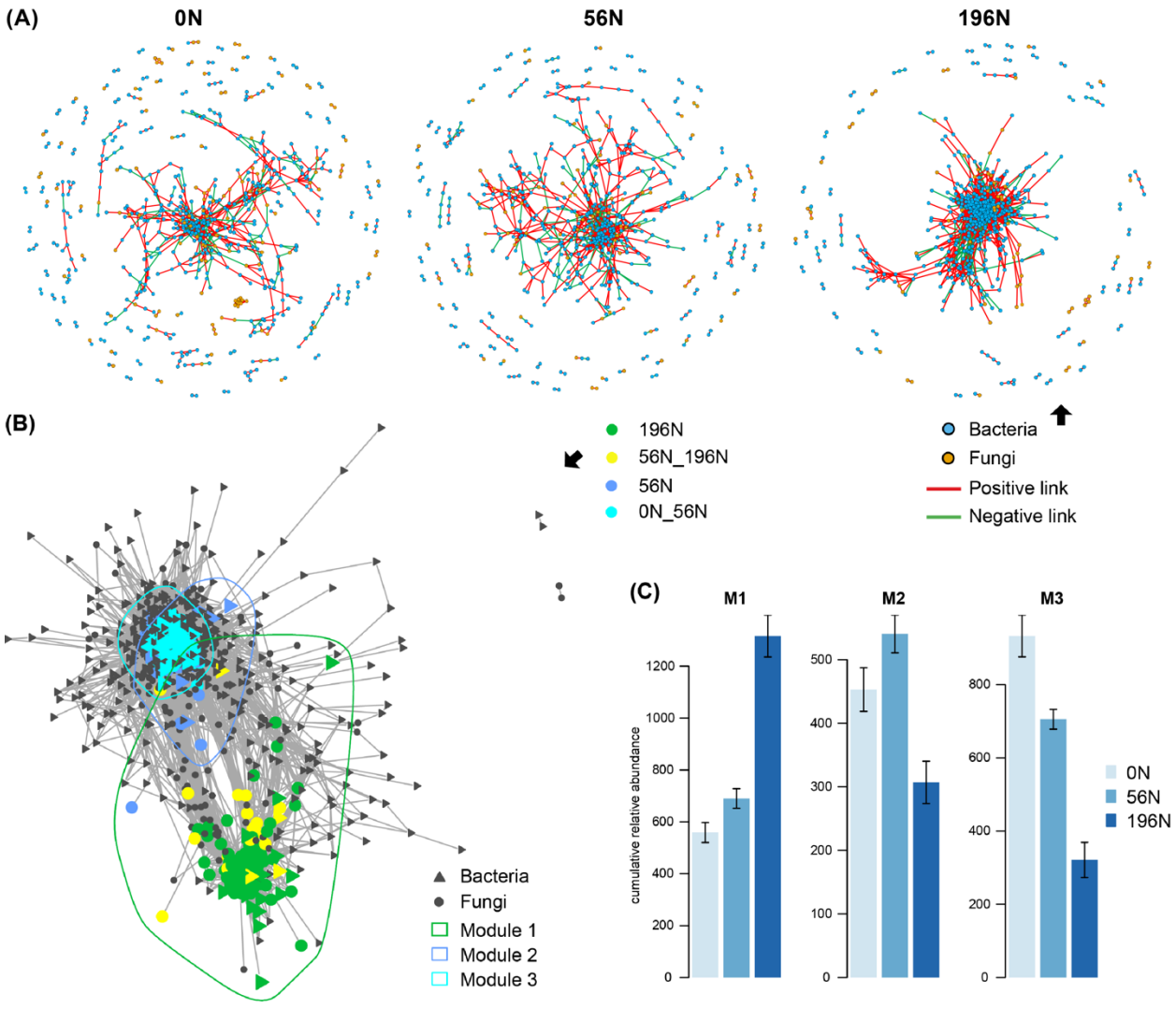
(A)
0N
56N
196N
(B)
196N
56N_196N
56N
0N_56N
Bacteria
Fungi
Positive link
Negative link
Bacteria
Fungi
Module 1
Module 2
Module 3
(C)
M1
M2
M3
cumulative relative abundance
0N
56N
196N

Fig. 3

935

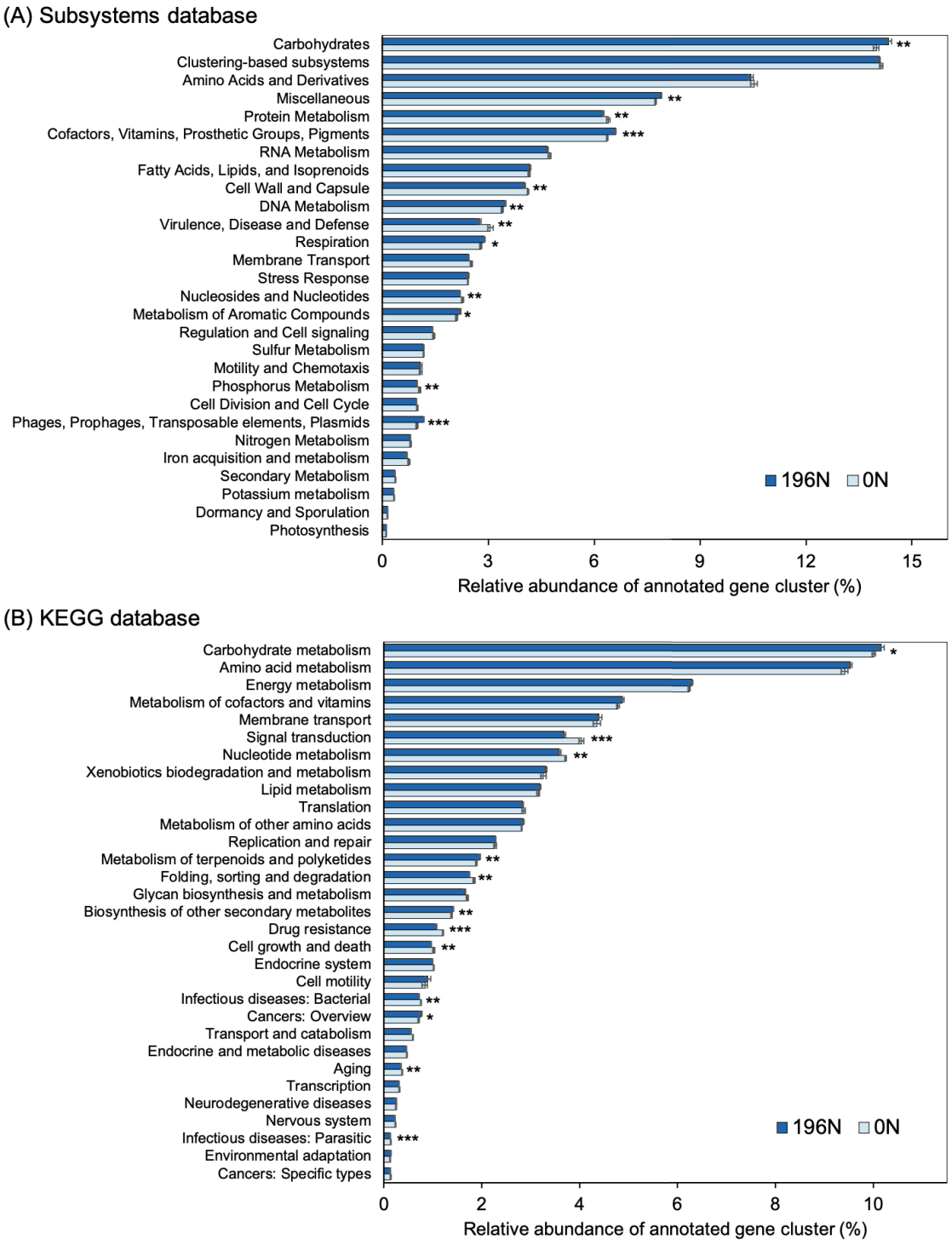

936

937 **Fig. 4**

938

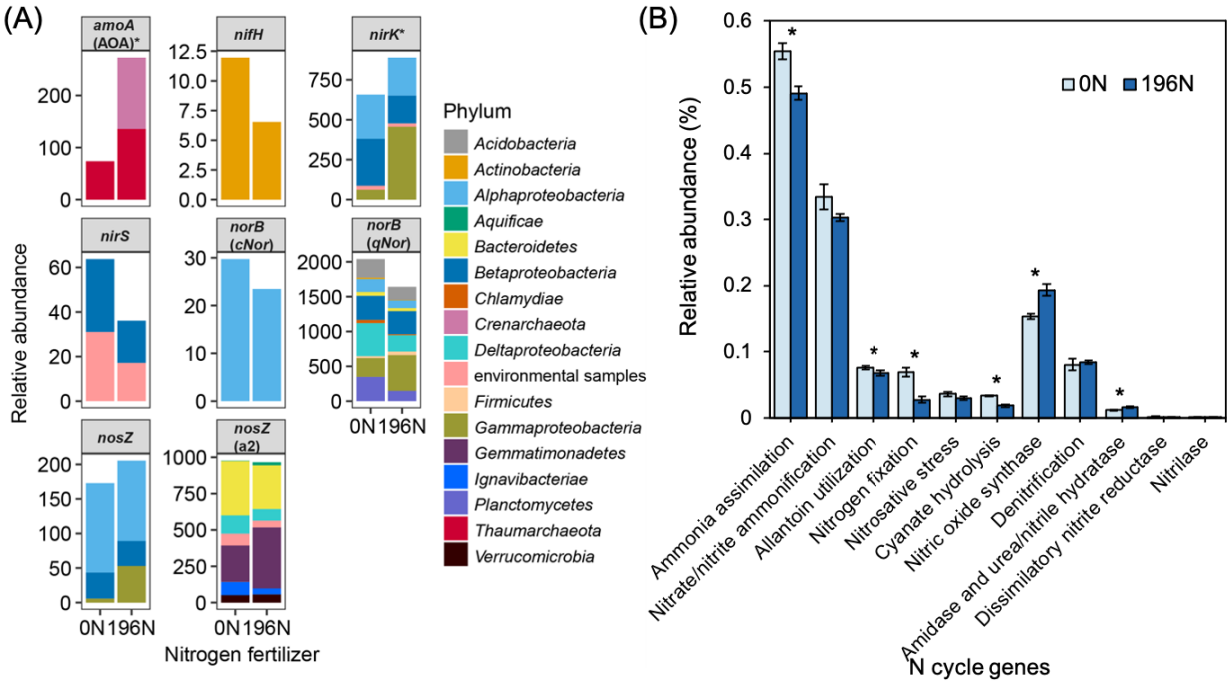

939

940 **Fig. 5**

Supplementary information

Long-term excess nitrogen fertilizer increases sensitivity of soil microbial community to seasonal change revealed by ecological network and metagenome analyses

Bing-Bing Li[a, b, c, d], Sarah S. Roley[e,g], David S. Duncan[f], Jiarong Guo[c, d], John F. Quensen[c, d], Han-Qing Yu[b, *] and James M. Tiedje[c, d, *]

[a] School of Life Sciences, University of Science & Technology of China, Hefei 230026, China

[b] CAS Key Laboratory of Urban Pollutant Conversion, Department of Chemistry, University of Science & Technology of China, Hefei 230026, China

[c] Department of Plant, Soil and Microbial Sciences, Michigan State University, East Lansing, Michigan 48824, USA

[d] Center for Microbial Ecology, Michigan State University, East Lansing, Michigan 48824, USA

[e] Great Lakes Bioenergy Research Center and W.K. Kellogg Biological Station, Michigan State University, Hickory Corners, Michigan 49060, USA

[f] Department of Agronomy, University of Wisconsin, Madison, Wisconsin 53706, USA

[g] Current address: School of the Environment, Washington State University, Richland WA 99354

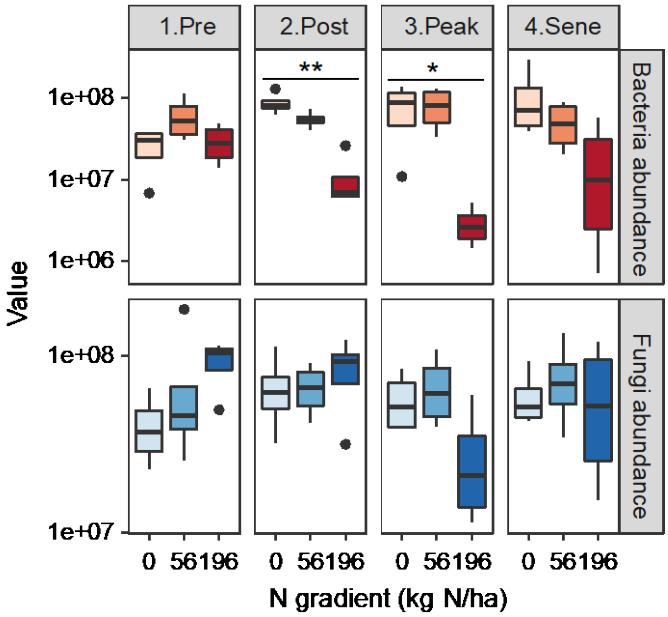

Fig. S1. 16S rRNA gene and ITS2 gene copy numbers for bacteria and fungi, respectively.

Significance: *$P < 0.05$, **$P < 0.01$.

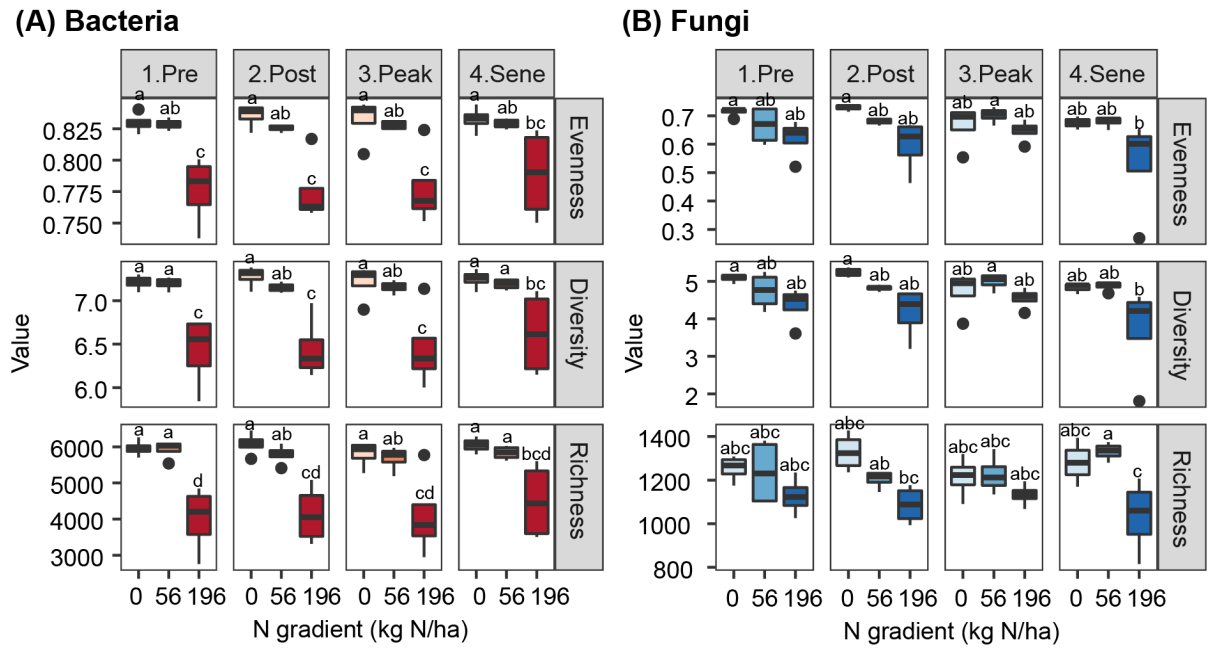

Fig. S2. Alpha diversities of bacterial community (A) and fungal community (B) across N gradient. Three alpha diversity indexes (Pielou's evenness, Shannon diversity and Species richness) were analyzed. 0N, 56N, and 196N represent different N fertilizer rates. Pre, post, peak, and sene refer to four growth stages, which are pre-fertilization, post-fertilization, peak productivity, and senescence, respectively. Letters indicate the ANOVA grouping among samples ($\alpha = 0.05$).

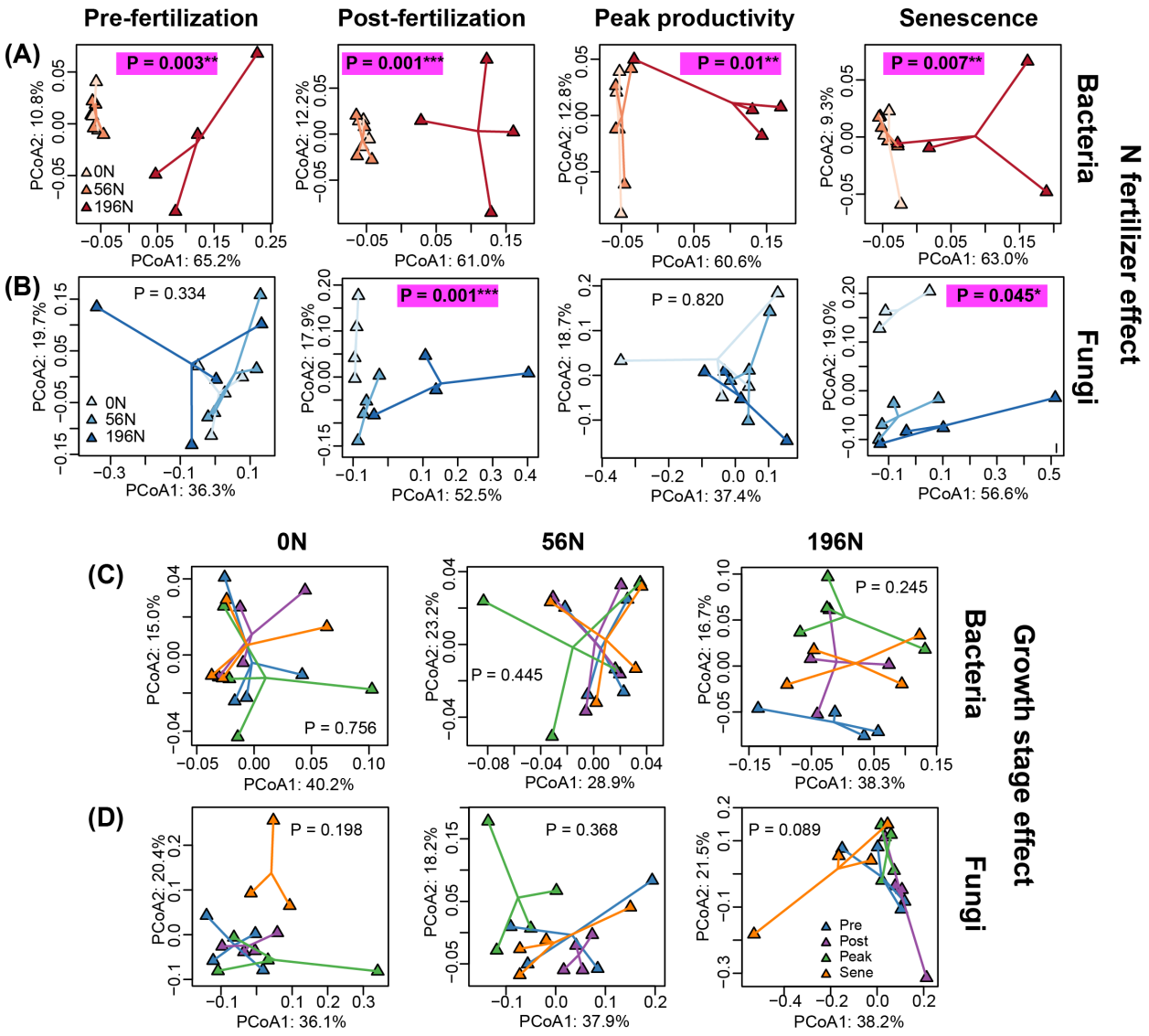

Fig. S3. Beta diversities of bacterial communities (A, C) and fungal communities (B, D) for each fertilizer rate or each growth stage. Principal coordinates analysis (PCoA) based on weighted UniFrac distance was adopted to analyze beta diversity. 0N, 56N and 196N represent different N fertilizer rates. Pre, Post, Peak and Sene represent four growth stages, which are pre-fertilization, post-fertilization, peak productivity and senescence, respectively. *$P < 0.05$, **$P < 0.01$, ***$P < 0.001$ indicate that the microbial communities were significantly different among treatments and are highlighted in pink boxes.

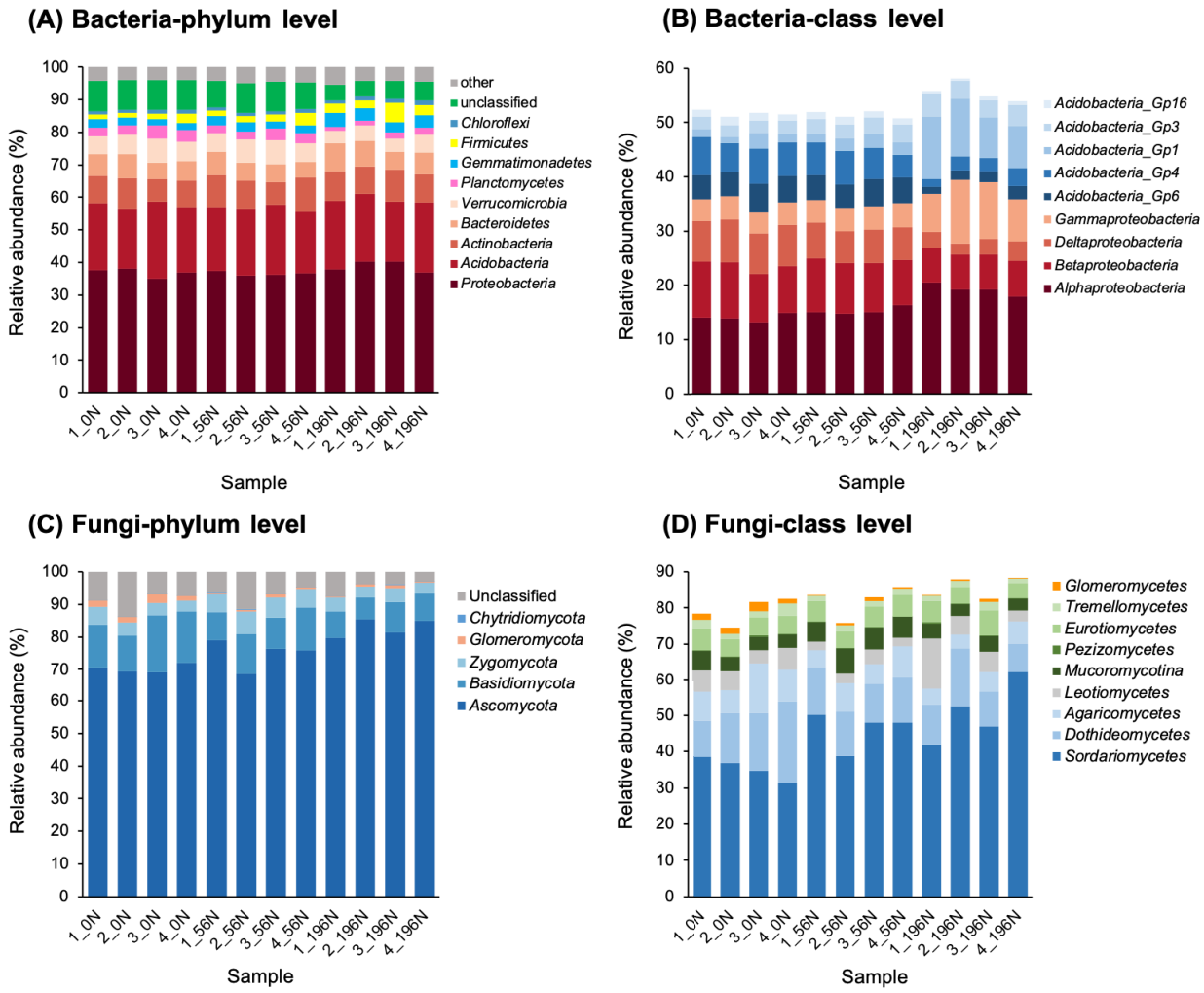

Fig. S4. Relative abundances of top bacterial phyla (A), some bacterial classes (B), all fungal phyla (C), and top fungal classes (D) across N fertilizer gradient during the growth of switchgrass. 1, 2, 3, 4 represent four growth stages. 0N, 56N, and 196N represent different N fertilizer rates.

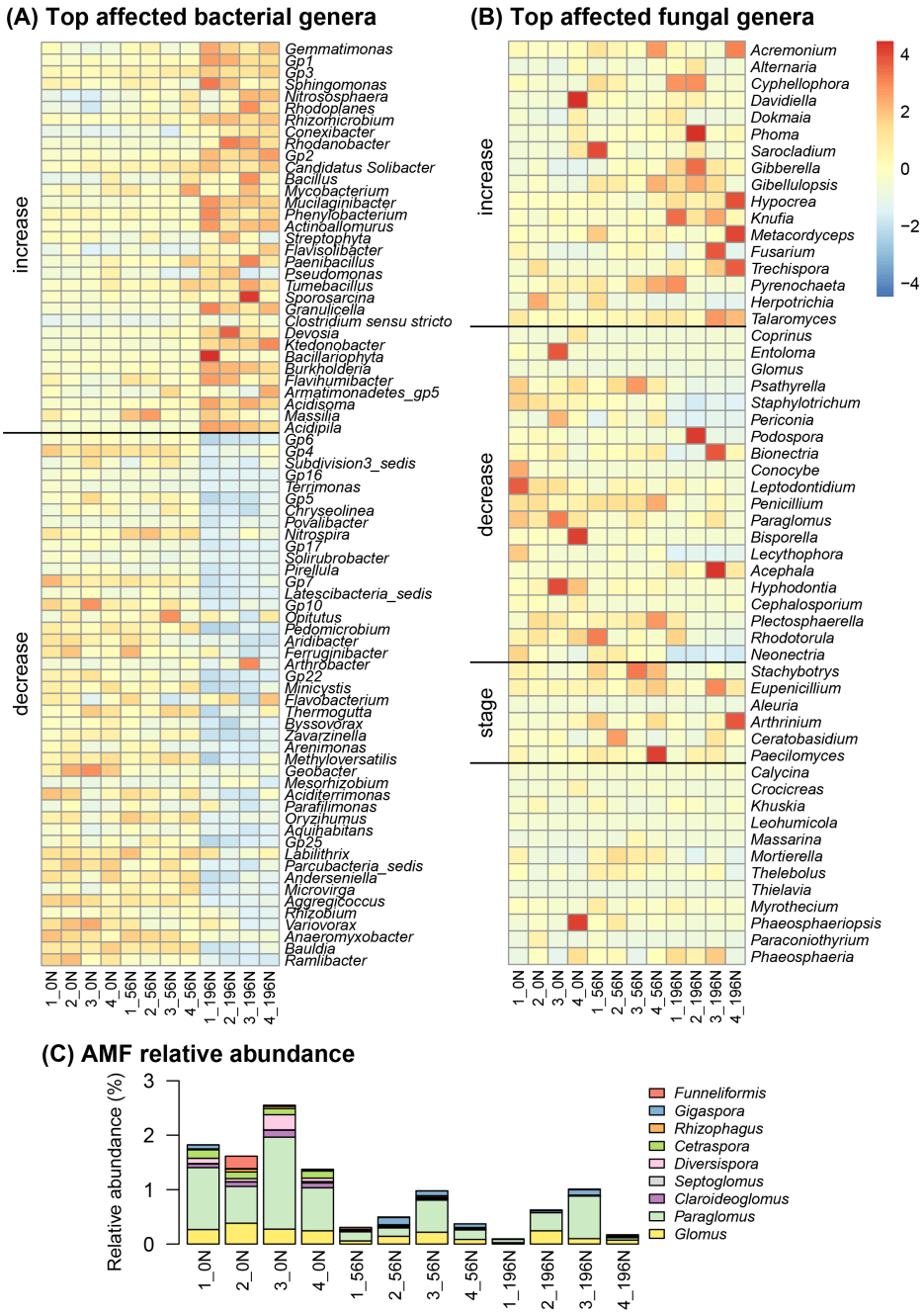

Fig. S5. Significantly affected bacterial genera (A), fungal genera (B) and arbuscular mycorrhiza fungi (C) by N fertilizer or growth stage. The "increase" and "decrease" indicate that corresponding genera were increased or decreased by N fertilizer. Fungal genera that were significantly affected by N fertilizer were also significantly affected by growth stage. The "stage" indicated that some fungal genera were only influenced by growth stage, not N fertilizer.

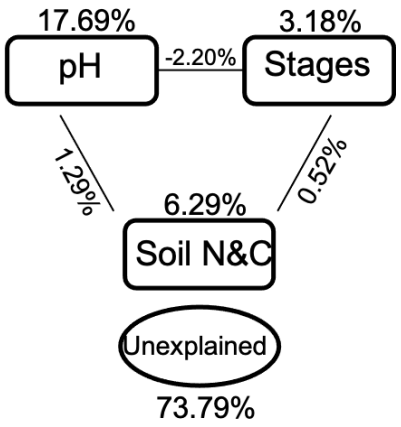

Fig. S6. Bray-Curtis dissimilarities based on variation partitioning analysis of microbial community structures explained by soil pH, soil N&C and growth stage based on OTU table. Soil N&C parameters include total C and N, ammonium, and nitrate.

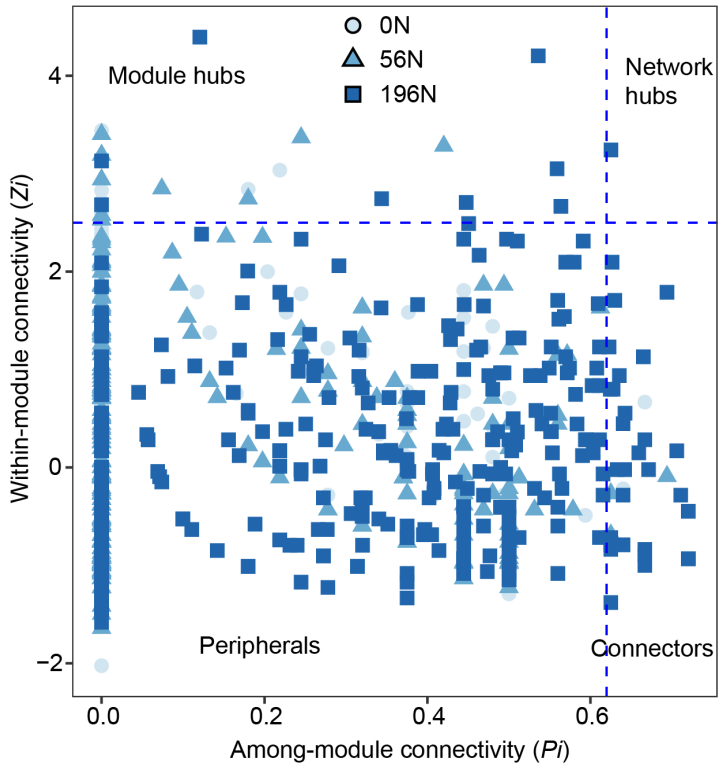

Fig. S7. Classification of nodes to identify putative keystone species within the networks based on *Pi* and *Zi* values. Each symbol represents an OTU. Nodes with $Zi > 2.5$ and $Pi > 0.62$ are network hubs. Nodes with $Zi > 2.5$ are module hubs. Nodes with $Pi > 0.62$ are connectors. Nodes with $Zi < 2.5$ and $Pi < 0.62$ are peripherals.

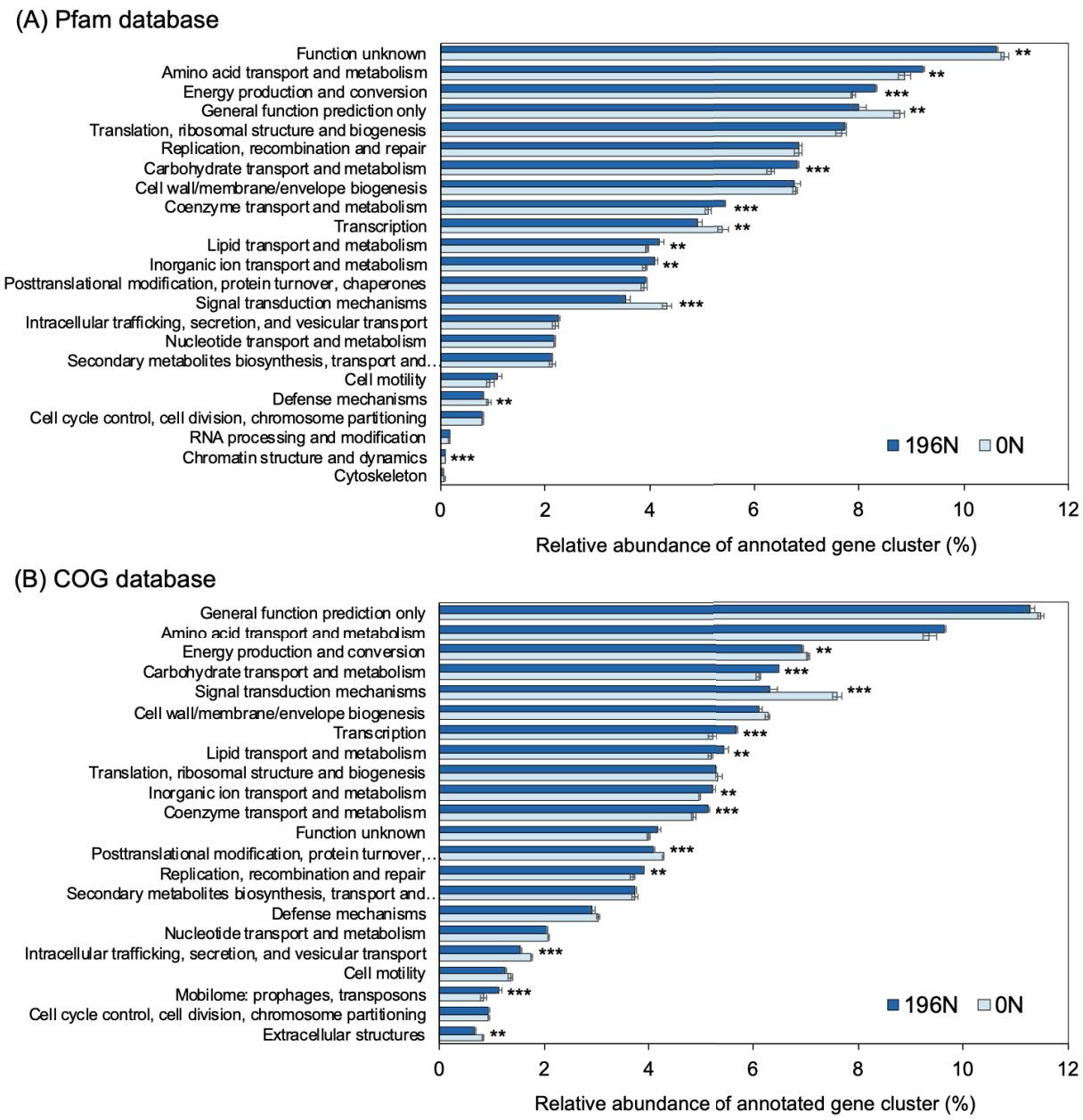

Fig. S8. Relative abundance of grouped function genes annotated based on Pfam database (A) and COG database (B) in 0N and 196N samples from peak productivity stage. Significance: **P* < 0.05, ***P* < 0.01, ****P* < 0.001.

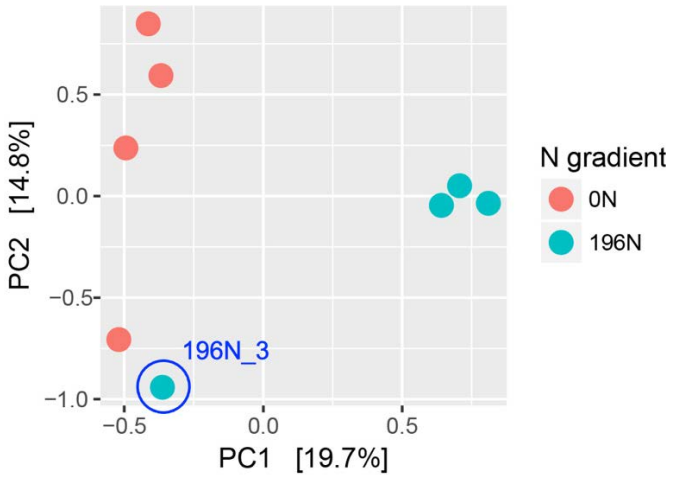

Fig. S9. Principal component analysis of bacterial community based on *rplB* gene for 0N and 196N samples from peak productivity stage. The circled data point was classified as an outlier and removed from subsequent analyses.

Table S1 Temperature, precipitation, ammonium, nitrate concentrations and pH value during the switchgrass growth for each N fertilizer rate

Growth stage		Pre-fertilization	Post-fertilization	Peak productivity	Senescence
Monthly average temperature (°C)		16.2	19.1	20.8	10.8
Monthly total precipitation (mm)		138	268	147	62
Mean annual temperature (°C)		9.2			
Mean annual precipitation (mm)		1,154			
Total carbon (%)	0N				0.85 ± 0.20^{b}
	56N				0.89 ± 0.13^{b}
	196N				0.80 ± 0.13^{b}
Total nitrogen (%)	0N				0.09 ± 0.04^{b}
	56N				0.08 ± 0.01^{b}
	196N				0.08 ± 0.01^{b}
Ammonium (ppm)	0N	0.31 ± 0.08^{b}	0.35 ± 0.08^{b}	0.35 ± 0.10^{b}	0.27 ± 0.05^{b}
	56N	0.27 ± 0.14^{b}	0.40 ± 0.11^{b}	0.30 ± 0.03^{b}	0.22 ± 0.02^{b}
	196N	0.19 ± 0.08^{b}	4.58 ± 1.79^{a}	0.24 ± 0.04^{b}	0.20 ± 0.07^{b}
Nitrate (ppm)	0N	0.20 ± 0.11^{b}	0.17 ± 0.02^{b}	0.09 ± 0.04^{b}	0.10 ± 0.05^{b}
	56N	0.26 ± 0.02^{b}	0.73 ± 0.16^{b}	0.24 ± 0.26^{b}	0.30 ± 0.13^{b}
	196N	0.15 ± 0.08^{b}	1.89 ± 1.45^{a}	0.27 ± 0.14^{b}	0.88 ± 0.22^{ab}
pH	0N	6.35 ± 0.20^{a}	6.35 ± 0.20^{a}	5.74 ± 0.13^{ab}	5.78 ± 0.09^{ab}
	56N	6.03 ± 0.24^{ab}	6.03 ± 0.24^{ab}	5.49 ± 0.25^{bcd}	5.58 ± 0.34^{abc}
	196N	4.93 ± 0.24^{cde}	4.93 ± 0.24^{cde}	4.79 ± 0.70^{de}	4.50 ± 0.28^{e}

Letters indicate the ANOVA grouping among fertilizer rates over four growth stages for each edaphic factor ($\alpha = 0.05$).

Table S2 Spearman correlation between alpha diversity index and soil properties

	Bacteria			Fungi		
	H diversity	J evenness	S richness	H diversity	J evenness	S richness
H diversity		0.98***	0.95***		0.99***	0.67***
J evenness			0.90***			0.56***
pH	0.68***	0.65***	0.72***	0.71***	0.69***	0.51***
Ammonium	0.17	0.21	0.11	0.08	0.07	0.11
Nitrate	-0.29*	-0.33*	-0.24	-0.24	-0.22	-0.23

Table S3 Effects of fertilization, growth stage and their interaction on bacterial community structures based on Unifrac distance through PERMANOVA analysis

	Fertilization		Season		Fertilization * Season	
	F	R^2	F	R^2	F	R^2
all	15.3***	0.41	0.70	0.05	1.05	0.08
Pre-fertilization	5.82**	0.56				
Post-fertilization	6.48***	0.59				
Peak productivity	4.04**	0.47				
Senescence	3.00**	0.40				
0N			0.79	0.16		
56N			1.01	0.20		
196N			1.20	0.23		

Table S4 Effects of fertilization, growth stage and their interaction on fungal community structures based on Unifrac distance through PPERMANOVA analysis

	Fertilization		Season		Fertilization * Season	
	F	R^2	F	R^2	F	R^2
All	3.22***	0.13	1.35	0.10	1.20	0.13
Pre-fertilization	1.09	0.19				
Post-fertilization	4.13***	0.48				
Peak productivity	0.73	0.14				
Senescence	1.97*	0.33				
0N			1.28	0.26		
56N			1.05	0.21		
196N			1.43	0.26		

Table S5 Lineages and relative abundances of connectors in each network

Connectors	Domain	Phylum	Class or order	Relative abundance (%)
0N	*Bacteria*	*Firmicutes*	*Clostridia*	0.055
	Bacteria	*Verrucomicrobia*	*Subdivision3*	0.074
56N	*Bacteria*	*Actinobacteria*	*Actinobacteria*	0.047
	Bacteria	*Acidobacteria*	*Acidobacteria_Gp6*	0.013
	Bacteria	*Acidobacteria*	*Acidobacteria_Gp4*	0.212
196N	*Bacteria*	*Proteobacteria*	*Alphaproteobacteria*	0.071
	Bacteria	*Acidobacteria*	*Acidobacteria_Gp1*	0.378
	Bacteria	*Actinobacteria*	*Actinobacteria*	0.015
	Bacteria	*Acidobacteria*	*Acidobacteria_Gp1*	0.020
	Bacteria	*Proteobacteria*	*Betaproteobacteria*	0.097
	Bacteria	*Acidobacteria*	*Acidobacteria_Gp3*	0.423
	Bacteria	*Acidobacteria*	*Acidobacteria_Gp6*	0.018
	Bacteria	*Actinobacteria*	*Actinobacteria*	0.098
	Bacteria	*Acidobacteria*	*Acidobacteria_Gp4*	0.017
	Bacteria	*Actinobacteria*	*Actinobacteria*	0.348
	Bacteria	*Proteobacteria*	*Alphaproteobacteria*	0.099
	Bacteria	*Chloroflexi*	*Anaerolineae*	0.038
	Bacteria	*Gemmatimonadetes*	*Gemmatimonadetes*	0.044
	Bacteria	*Planctomycetes*	*Planctomycetia*	0.112
	Bacteria	*Acidobacteria*	*Acidobacteria_Gp5*	0.022
	Bacteria	*Bacteroidetes*	*Sphingobacteriia*	**0.658**
	Bacteria	*Planctomycetes*	*Planctomycetia*	0.019
	Bacteria	*Proteobacteria*	*Alphaproteobacteria*	0.011
	Bacteria	*Acidobacteria*	*Acidobacteria_Gp2*	0.322
	Bacteria	*Proteobacteria*	*Deltaproteobacteria*	0.059
	Bacteria	*Proteobacteria*	*Deltaproteobacteria*	0.075
	Bacteria	*Proteobacteria*	*Deltaproteobacteria*	0.017
	Bacteria	*Acidobacteria*	*Acidobacteria_Gp4*	0.016
	Bacteria	***Proteobacteria***	***Betaproteobacteria***	**0.056**
	Bacteria	*Bacteroidetes*	*Sphingobacteriia*	0.016
	Bacteria	*Acidobacteria*	*Acidobacteria_Gp1*	**0.740**
	Bacteria	*Bacteroidetes*	*Sphingobacteriia*	0.013
	Bacteria	*Proteobacteria*	*Gammaproteobacteria*	0.019
	Bacteria	*Acidobacteria*	*Acidobacteria_Gp6*	0.054
	Bacteria	*Acidobacteria*	*Acidobacteria_Gp4*	0.186
	Bacteria	*Acidobacteria*	*Acidobacteria_Gp10*	0.013

Table S6 Lineages and relative abundances of module hubs in each network

Module hubs	Domain	Phylum	Class or order	Relative abundance (%)
0N	*Bacteria*	*Proteobacteria*	*Alphaproteobacteria*	0.067
	Bacteria	*Verrucomicrobia*	*Subdivision3*	0.032
	Bacteria	*Actinobacteria*	*Actinobacteria*	0.084
	Bacteria	*Proteobacteria*	*Alphaproteobacteria*	0.061
	Bacteria	*Proteobacteria*	*Alphaproteobacteria*	0.041
	Bacteria	*Bacteroidetes*	*Sphingobacteriia*	0.427
56N	*Bacteria*	*Acidobacteria*	*Acidobacteria_Gp4*	0.031
	Bacteria	*Acidobacteria*	*Acidobacteria_Gp7*	0.016
	Bacteria	*Acidobacteria*	*Acidobacteria_Gp3*	0.082
	Bacteria	*Verrucomicrobia*	*Subdivision3*	0.072
	Bacteria	*Acidobacteria*	*Acidobacteria_Gp3*	0.285
	Bacteria	*Acidobacteria*	*Acidobacteria_Gp4*	0.052
	Bacteria	*Bacteroidetes*	*Sphingobacteriia*	0.023
	Bacteria	*Gemmatimonadetes*	*Gemmatimonadetes*	0.012
	Fungi	*Ascomycota*	*Sordariomycetes*	0.431
	Fungi	*Zygomycota*	*Mucoromycotina_Incertae_sedis*	0.343
196N	*Bacteria*	*Proteobacteria*	*Gammaproteobacteria*	0.117
	Bacteria	*Acidobacteria*	*Acidobacteria_Gp6*	0.151
	Bacteria	***Proteobacteria***	***Betaproteobacteria***	**0.056**
	Bacteria	*Firmicutes*	*Bacilli*	**0.638**
	Bacteria	*Bacteroidetes*	*Sphingobacteriia*	0.109
	Bacteria	*Acidobacteria*	*Acidobacteria_Gp1*	0.224
	Bacteria	*Acidobacteria*	*Acidobacteria_Gp6*	0.129
	Bacteria	*Firmicutes*	*Bacilli*	0.086
	Bacteria	*Proteobacteria*	*Betaproteobacteria*	0.070